Shortcuts to Adiabaticity for Open Quantum Systems and a Mixed-State Inverse Engineering Scheme

S.L. Wu[1,*], W. Ma,[1] X.L. Huang,[2] and Xuexi Yi[3,†]

[1] *School of Physics and Materials Engineering, Dalian Nationalities University, Dalian 116600, China*
[2] *School of Physics and Electronic Technology, Liaoning Normal University, Dalian 116029, China*
[3] *Center for Quantum Sciences and School of Physics, Northeast Normal University, Changchun 130024, China*

We propose a fast mixed-state control scheme to transfer the quantum state along designable trajectories in Hilbert space, which is robust to multiple decoherence noises. Starting with the dynamical invariants of open quantum systems, we present the shortcuts to adiabaticity (STA) of open quantum systems at first, then apply the STA to speed up the adiabatic steady process. Our scheme drives open systems from a initial steady state to a target steady state by a controlled Liouvillian that possesses the same form as the reference (original) one that is accessible in present-day experiments. An experimental design with currently available parameters for the nitrogen-vacancy (N-V) center in diamond is suggested and discussed.

I. INTRODUCTION

Controlling quantum systems to accomplish a special task is at the heart of emerging quantum technologies [1–3]. The ideal control scheme needs to satisfy three important issues. (i) High speed: the quantum state transfers to the target state within the desired control time length. (ii) High fidelity: the control process should be with an admissible error. (iii) High controllability: the trajectory from an initial state to a target state must be completely controllable.

The most selected schemes in experiment are based on the unitary evolution of closed systems [4–7]. Yet unwanted couplings to the environment severely reduce the fidelity [8,9], and the final state cannot be steadied on the target state after the control is done. This shackles the quantum sciences and technologies to realize efficient and scalable devices beyond the current circumstances of proof-of-principle demonstrations. To overcome such shackles, a straightforward thinking is to formulate a scheme based on the theory of open quantum systems. Because of its steadiness, the steady state becomes an important candidate for achieving the quantum control task [10]. The adiabatic steady-state engineering scheme transfers the quantum state into the target state along the instantaneous steady state [11,12]. But the control process needs to be very slow so that the adiabatic condition can be satisfied. Also, fast steady-state engineering schemes are proposed to accelerate the adiabatic evolution of the

equilibrium state of the quantum thermodynamic system, which can only be applied to the Gibbs states or the Gaussian states [13,14]. On the other hand, the transitionless quantum driving method of open quantum systems is also proposed, but a feasible control protocol is hard to present [15,16]. Therefore, up to the present day, none of schemes satisfy the requirements of high accuracy, high controllability, and high speed at the same time.

In this paper, we propose a fast control scheme for open quantum systems, named the mixed-state inverse engineering (MIE) scheme, which allows a robust and precise transfer to a given target state with a designable mixed state trajectory. Firstly, by analyzing the spectral features of dynamical invariant superoperators of open quantum systems [17], we present general solutions of quantum states governed by the master equation

$$\partial_t |\rho(t)\rangle\rangle = \hat{\mathcal{L}}_c(t)|\rho(t)\rangle\rangle \tag{1}$$

with the Liouvillian superoperator $\hat{\mathcal{L}}_c(t)$. Based on this general solution, the STA of open quantum systems are established. Then, we apply the STA of open quantum systems to steady-state engineering (i.e., the MIE scheme) and show that the target state can be reached with extremely high fidelity and within the desired control time length. The main advantage of our scheme is that the control tasks are, in general, achieved with fruitful feasible control protocols in experiment by selecting different quantum state trajectories. More importantly, the selectable trajectories can lead to the ideal final fidelity even when multiple noise sources are involved. In fact, the pure-state inverse engineering scheme of closed quantum systems is a particular

---

*slwu@dlnu.edu.cn
†yixx@nenu.edu.cn

case of the STA scheme of open quantum systems [18], when the trajectories of quantum states are the pure-state trajectories. Also, the MIE scheme can overcome the difficulties of earlier STA methods for closed systems due to the designable mixed-state trajectory.

The rest of this paper is organized as follows. In Sec. II, we present the STA scheme of open quantum systems, and propose the MIE scheme to accelerate the adiabatic steady-state process. In Sec. III, we apply the MIE scheme to the N-V center system, which provides simple, practical, robust control protocols to transfer the population from one ground state to the other [19,20]. It is shown that the MIE scheme is far better at transferring efficiency than any STA scheme of closed systems [9], especially in the case that the three-level system suffers from dissipation and dephasing at the same time. In Sec. IV, we discuss the relationship between the mixed-state inverse engineering scheme and the pure-state inverse engineering scheme of closed systems [18]. Conclusions are presented in Sec. V.

II. METHODS

A. STA of open quantum systems

For an open quantum system governed by Eq. (1), a dynamical invariant of the open quantum system is defined as a superoperator $\hat{\mathcal{I}}(t)$ that satisfies [17]

$$\partial_t \hat{\mathcal{I}}(t) - [\hat{\mathcal{L}}_c(t), \hat{\mathcal{I}}(t)] = 0. \tag{2}$$

In general, invariants are non-Hermitian. Thus, $\hat{\mathcal{I}}(t)$ needs to be expressed in Jordan canonical form. Consider that there are m Jordan blocks and that the αth Jordan block is n_α dimensional. According to the Jordan decomposition of $\hat{\mathcal{I}}(t)$, we introduce right vectors $\{|D_\alpha^{(i)}\rangle\rangle\}$ and left vectors $\{\langle\langle E_\alpha^{(i)}|\}$ in the Hilbert-Schmidt space. The left and right vectors always satisfy

$$\hat{\mathcal{I}}|D_\alpha^{(i)}\rangle\rangle = \lambda_\alpha|D_\alpha^{(i)}\rangle\rangle + |D_\alpha^{(i-1)}\rangle\rangle,$$
$$\langle\langle E_\alpha^{(i)}|\hat{\mathcal{I}} = \lambda_\alpha\langle\langle E_\alpha^{(i)}| + \langle\langle E_\alpha^{(i+1)}|,$$

with $|D_\alpha^{(-1)}\rangle\rangle \equiv 0, \langle\langle E_\alpha^{(n_\alpha)}| \equiv 0,$ for $i = 0, 1, \ldots, n_\alpha - 1$. Thus, the right and left vectors $|D_\alpha^{(0)}\rangle\rangle$ and $\langle\langle E_\alpha^{(n_\alpha-1)}|$ are the right and left eigenstates of $\hat{\mathcal{I}}(t)$ with the eigenvalue λ_α. Here we assume that all of eigenvalues are nondegenerate, i.e., $\lambda_\alpha \neq \lambda_\beta$ for all $\alpha \neq \beta$. Also, the left and right vectors satisfy the orthonormality condition

$$\langle\langle E_\alpha^{(i)}|D_\beta^{(j)}\rangle\rangle = \delta_{\alpha\beta}\delta_{ij}.$$

It can be verified that the eigenvalues of the dynamical invariants are time independent, and that

$$\langle\langle E_\beta^{(j)}|\hat{O}|D_\alpha^{(i)}\rangle\rangle = 0 \quad \text{for all } i,j$$

with $\hat{O} = \hat{\mathcal{L}} - \partial_t$ for $\alpha \neq \beta$. Therefore, it can be verified that the general solution of Eq. (1) reads

$$|\rho(t)\rangle\rangle = \sum_{\alpha=0}^{m-1} c_\alpha \exp[\eta_\alpha(t)]|\Phi_\alpha(t)\rangle\rangle, \tag{3}$$

in which $\eta_\alpha(t)$ is a complex phase, c_α is a time-independent expansion efficient, and $|\Phi_\alpha(t)\rangle\rangle$ is a right vector in the αth Jordan block, which can be written as

$$|\Phi_\alpha(t)\rangle\rangle = \sum_{i=0}^{n_\alpha-1} b_i^\alpha(t)|D_\alpha^{(i)}(t)\rangle\rangle \tag{4}$$

with coefficients $b_i^\alpha(t)$. The details of the derivation of the general solution Eq. (3) can be found in Appendix A.

Since the adiabaticity of open quantum systems requires only forbidding the transition between different Jordan blocks [10], the general solution, Eq. (3), is enough to establish STA of open quantum systems. Suppose that our aim is to drive the quantum system from an initial Liouvillian $\hat{\mathcal{L}}_c(0)$ to a final one, $\hat{\mathcal{L}}_c(t_f)$, such that the "populations" in the initial and final instantaneous Jordan blocks are the same but admit transitions at intermediate times. Based on the general solution, Eq. (3), the complex phases $\eta_\alpha(t)$ are chosen as arbitrary functions such that the time-evolution superoperator $\hat{\mathcal{E}}(t)$ can be written as

$$\hat{\mathcal{E}}(t) = \sum_{\alpha=0}^{m-1} \exp[\eta_\alpha(t)]|\Phi_\alpha(t)\rangle\rangle\langle\langle\Psi_\alpha(0)|,$$

where $\langle\langle\Psi_\alpha(t)|$ is a left vector of the αth Jordan block, which satisfies $\langle\langle\Psi_\beta(t)|\Phi_\alpha(t)\rangle\rangle = \delta_{\alpha\beta}$. The evolution superoperator obeys

$$\partial_t \hat{\mathcal{E}}(t) = \hat{\mathcal{L}}_c(t)\hat{\mathcal{E}}(t),$$

which we formally solve for the control Liouvillian

$$\hat{\mathcal{L}}_c(t) = \partial_t \hat{\mathcal{E}}(t)\hat{\mathcal{E}}^{-1}(t)$$

with

$$\hat{\mathcal{E}}^{-1}(t) = \sum_{\alpha=0}^{m-1} \exp[-\eta_\alpha(t)]|\Phi_\alpha(0)\rangle\rangle\langle\langle\Psi_\alpha(t)|.$$

Thus, we can express the control Liouvillian superoperator as

$$\hat{\mathcal{L}}_c(t) = \sum_{\alpha=0}^{m-1} [|\partial_t\Phi_\alpha(t)\rangle\rangle\langle\langle\Psi_\alpha(t)|$$
$$+ \partial_t\eta_\alpha(t)|\Phi_\alpha(t)\rangle\rangle\langle\langle\Psi_\alpha(t)|]. \tag{5}$$

Note that, for a given dynamical invariant, there are many possible Liouvillians corresponding to different choices of

complex phases $\eta_\alpha(t)$. In general, $\hat{\mathcal{I}}(0)$ does not commute with $\hat{\mathcal{L}}_c(0)$, which implies that the Jordan blocks of $\hat{\mathcal{I}}(0)$ do not coincide with the Jordan blocks of $\hat{\mathcal{L}}_c(0)$. Here $\hat{\mathcal{L}}_c(t_f)$ does not necessarily commute with $\hat{\mathcal{I}}(t_f)$ either. We impose $[\hat{\mathcal{I}}(0), \hat{\mathcal{L}}_c(0)] = [\hat{\mathcal{I}}(t_f), \hat{\mathcal{L}}_c(t_f)] = 0$, such that the Jordan blocks coincide and then the quantum state transfer from the initial block to the final one is guaranteed. Here, we must emphasize that $|\Phi_\alpha(t)\rangle\rangle$ can be an arbitrary superposition of the right basis vectors $\{|D_\alpha^{(i)}(t)\rangle\rangle\}_{i=0}^{n_\alpha-1}$ for the αth Jordan block. In other words, if the quantum state is prepared in a given Jordan block of $\hat{\mathcal{L}}_c(0)$ at the beginning and the final state is still in the same block of $\hat{\mathcal{L}}_c(t_f)$, the shortcuts to adiabaticity of open quantum systems is established, which is the control Liouvillian given by Eq. (5) designed to speed up the adiabatic evolution of open quantum systems [10]. This is the first result of this paper.

In Appendix B, we present a detailed comparison between the STA scheme and the transitionless quantum driving scheme of open quantum systems [15]. It is shown that, if the trajectory of the STA scheme of open quantum systems is chosen as the adiabatic trajectory, the STA scheme is coincident with the transitionless quantum driving method proposed in Ref. [15]. However, the adiabatic trajectory is not the only choice for the trajectories in our scheme. There are many trajectories that can be used to inversely engineer the open quantum system. Proper trajectories always provide reasonable and applicable control protocols, which helps us to overcome the difficulties met in the control of microscopic or/and mesoscopic systems.

B. Mixed-state inverse engineering

In a practical application, the general control Liouvillian presented in Eq. (5) will experience difficulties in giving practical and affirmatory control protocols. In addition, most of eigenvectors of the control Liouvllian $\hat{\mathcal{L}}_c(t)$ are nonphysical quantum states, except the eigenvectors with zero eigenvalues, which correspond to steady states of open quantum systems. Therefore, for practical applications, we focus our attention on the steady-state engineering of open quantum systems. Even if we restrict our discussion to speeding up the adiabatic steady-state process, it is still difficult to obtain feasible control protocols [16], since the control Liouvillian given in Eq. (5) is in superoperator form. In the following, we propose an effective and practical method to obtain feasible control protocols, which is easy to use in experiment.

We consider a quantum system with N-dimensional Hilbert space governed by a linear, time-local master equation

$$\partial_t \rho(t) = \hat{\mathcal{L}}_0(t)[\rho(t)]$$
$$= -\frac{i}{\hbar}[H_0(t), \rho] + \sum_\alpha \hat{\mathcal{D}}[L_\alpha](\rho),$$

where $\hat{\mathcal{L}}_0(t)$ is the reference Liouvillian in Lindblad form, $H_0(t)$ is the Hamiltonian, and

$$\hat{\mathcal{D}}[L_\alpha](\rho) = L_\alpha(N_\alpha)\rho L_\alpha^\dagger(N_\alpha) - \tfrac{1}{2}\{L_\alpha^\dagger(N_\alpha)L_\alpha(N_\alpha), \rho\} \quad (6)$$

is the Lindbladian. The Lindblad operators $L_\alpha(N_\alpha)$ are related to some parameters $\{N_\alpha\}$, such as the decoherence rates and the temperatures of the environments. Here, we do not limit the master equation to be Markovian, but the corresponding evolution must be a completely positive trace-preserving map. Furthermore, we assume that $\hat{\mathcal{L}}_0(t)$ admits a unique (instantaneous) steady state $\rho_0(t)$, which satisfies

$$\hat{\mathcal{L}}_0(t)[\rho_0(t)] = 0.$$

For practical applications, we focus our attention on speeding up the adiabatic steady-state process [11], and seek the control Liouvillian from Eq. (2) directly. Concretely, the control task is to drive the open quantum system from the steady state of an initial Liouvillian $\hat{\mathcal{L}}_0(0)$ to the target one, $\hat{\mathcal{L}}_0(t_f)$ [10,11]. To this end, we consider that the invariant has only one one-dimensional Jordan block with nonzero eigenvalue Ω_I. If we set $|\Phi_0(0)\rangle\rangle = |\rho_0(0)\rangle\rangle$ and $|\Phi_0(t_f)\rangle\rangle = |\rho_0(t_f)\rangle\rangle$, the eigenvector $|\Phi_0(t)\rangle\rangle$ corresponds to the trajectory connecting the initial steady state and the target steady state. In general, we need to parameterize $\hat{\mathcal{I}}(t)$ in N^2-dimensional Hilbert-Schmidt space with N^4 independent coefficients [16]. For the MIE scheme, since $|\Phi_0(t)\rangle\rangle$ should be a quantum state of the open quantum system, we can expand $|\Phi_0(t)\rangle\rangle$ by right vectors $\{|T_\mu\rangle\rangle\}_{\mu=1}^{N^2-1}$ that correspond to SU(N) Hermitian generators $\{T_\mu\}_{\mu=1}^{N^2-1}$, i.e.,

$$|\Phi_0(t)\rangle\rangle = \frac{1}{N}\left(|I\rangle\rangle + \sqrt{\frac{N(N-1)}{2}}\sum_{\mu=1}^{N^2-1} r_\mu |T_\mu\rangle\rangle\right), \quad (7)$$

where $\vec{r} = (r_1, r_2, \ldots, r_{N^2-1})$ is the generalized Bloch vector with $\sum_\mu |r_\mu|^2 < 1$ and $|I\rangle\rangle$ is the right vector corresponding to an $N \times N$ identical operator. Thus, the dynamical invariants used in the MIE scheme can be defined as

$$\hat{\mathcal{I}}(t) = \Omega_I |\Phi_0(t)\rangle\rangle\langle\langle I|, \quad (8)$$

where Ω_I is an arbitrary nonzero constant and $\langle\langle I|$ is the left vector corresponding to an $N \times N$ identity matrix. With this notation, we can parameterize the dynamical invariant $\hat{\mathcal{I}}(t)$ with only $N^2 - 1$ parameters, which greatly simplifies the procedure in formulating control protocols.

To formulate feasible control protocols, we impose the condition that the control Liouvillians take the form

$$\hat{\mathcal{L}}_c[\bullet] = -\frac{i}{\hbar}[H(t), \bullet] + \sum_{\alpha} \hat{\mathcal{D}}[L_\alpha](\bullet), \qquad (9)$$

in which the Lindbladians and the Hamiltonian are chosen according to the following principles. (i) The Lindbladians in the control Liouvillian $\hat{\mathcal{L}}_c(t)$ have the same form as Eq. (6), which controls the system through control parameters $\{N_\alpha\}$. (ii) The control can also be exerted on the system via the Hamiltonian in $\hat{\mathcal{L}}_c(t)$. As it can be written in terms of SU(N) Hermitian generators $\{T_k\}$, i.e.,

$$H(t) = \sum_{k=1}^{N^2-1} c_k(t) T_k,$$

we might choose $\{c_k(t)\}$ as the control parameters to manipulate the system. In this way, the control Liouvillians can always present feasible control protocols. Substituting $\hat{\mathcal{L}}_c(t)$ and $\hat{\mathcal{I}}(t)$ into Eq. (2), we can express the control parameters $\{c_k, N_\alpha\}$ as a function of the generalized Bloch vector and its derivative $\{r_\mu, \partial_t r_\mu\}$. On the other hand, the control Liouvillian is always the same as the reference Liouvillian at the initial and final moments, which leads to boundary conditions for $\{r_\mu, \partial_t r_\mu\}$. By utilizing the control parameters $\{c_k, N_\alpha\}$ and setting proper boundary conditions for $\{r_\mu, \partial_t r_\mu\}$, the open quantum system can be transferred from the initial steady state into the target steady state along an exact trajectory given by $|\Phi_0(t)\rangle\rangle$. This is the second result of this paper.

If some control parameters, say $\{\tilde{c}_k, \tilde{N}_\alpha\}$, are difficult to implement in a real setting, we can single out the equations for those parameters, and force them to be some values that are available in the experimental setting. Note that the equations for $\{\tilde{c}_k, \tilde{N}_\alpha\}$ are about the components of the trajectory $\{r_\mu, \partial_t r_\mu\}$. Thus, choosing proper $\{\tilde{r}_\mu\}$ as special components in trajectory to restrict $\{\tilde{c}_k, \tilde{N}_\alpha\}$ to be the preset values, we obtain a set of differential equations about $\{\tilde{r}_\mu\}$. Solving those differential equations is equivalent to choosing a trajectory with particular components $\{\tilde{r}_\mu\}$. Therefore, the MIE scheme can avoid those difficulties encountered in the control process, such as the negative decoherence rate [21] and the impractical energy-level couplings [6]. As a result, the MIE scheme offers a practical method to engineer an open quantum system with an exact trajectory that can be realized in a laboratory with current technology.

III. EXAMPLE: THE STIMULATED RAMAN ADIABATIC PASSAGE

Consider a single nitrogen-vacancy (N-V) center in diamond, which hosts a solid-state Λ system. The N-V center
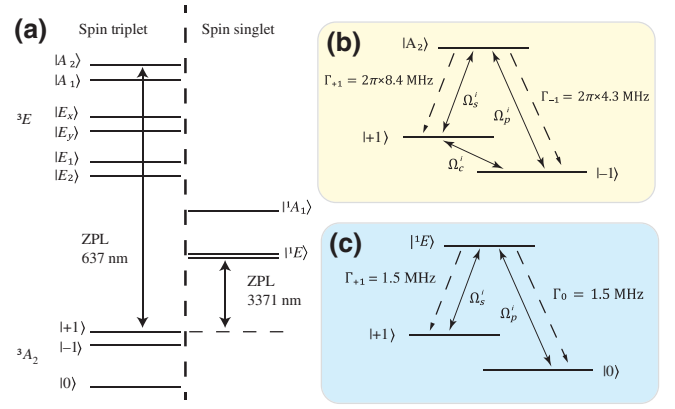

FIG. 1. The level structure of the N-V center. (a) A schematic illustration of the level structure of the N-V center. The optical zero photon line (ZPL) at 637 nm is related to the transition from ^3E to $^3A_2$ and the ZPL at 3371 nm corresponds to the transition from ^1E to $^3A_2$. (b) State transfer in a N-V center Λ system by the protocol with initial-to-final state coupling. (c) State transfer in a N-V center Λ system by the protocol without initial-to-final state coupling.

has a spin-triplet, orbital-singlet ground state ($^3A_2$) that is coupled optically to a spin-triplet, orbital-doublet excited state (^3E), as shown in Fig. 1(a). The experiments have identified the three singlet states ($|^1E\rangle$, $|^1A_1\rangle$) [22], where $|^1E\rangle$ is double degenerate.

For the negatively charged N-V center with electron spin $S = 1$, the ground state is a spin-triplet state with a zero-field splitting $D_0 = 2.87$ GHz between spin sublevels $|m_s = 0\rangle$ and $|m_s = \pm 1\rangle$ due to electronic spin-spin interaction. Applying a static magnetic field $B_{\text{N-}V}$ along the N-V axis splits the $|m_s = -1\rangle$ and $|m_s = +1\rangle$ ground states by $2\gamma_{\text{N-}V} B_{\text{N-}V}$ with $\gamma_{\text{N-}V} = 2.8$ MHz G^{-1}. Passing a single tunable laser (637.2 nm) through a phase electro-optic modulator causes frequency harmonics to resonantly excite both $|m_s = -1\rangle$ and $|m_s = +1\rangle$ to the spin-orbit excited state $|A_2\rangle$, which is used as the intermediate state for the stimulated Raman adiabatic passage (STIRAP). The modulation of an amplitude electro-optic modulator with a 10 GHz arbitrary wave form generator produces the control fields $\Omega_s(t)$ and $\Omega_p(t)$ used in STIRAP. The Hamiltonian within the rotating-wave approximation can be expressed in the basis $\{|m_s = -1\rangle, |A_2\rangle, |m_s = +1\rangle\}$ as a matrix [23]:

$$H_0(t) = \frac{\hbar}{2} \begin{pmatrix} 0 & \Omega_p(t) & 0 \\ \Omega_p(t) & 0 & \Omega_s(t) \\ 0 & \Omega_s(t) & 0 \end{pmatrix}. \qquad (10)$$

To simplify our discussion, the "one-photon resonance" case is considered. The shortcuts of the open STIRAP for a general case can be obtained with the same procedure. Here we assume that the adiabatic pulses satisfy

$$\Omega_s(t) = \Omega(t) \cos\theta(t), \qquad \Omega_p(t) = \Omega(t) \sin\theta(t), \quad (11)$$

with $\tan\theta(t) = \Omega_p(t)/\Omega_s(t)$ and $\Omega(t) = \sqrt{\Omega_s^2(t) + \Omega_p^2(t)}$.

Consider that the Λ system couples to a bosonic heat reservoir at finite temperature T. The effect of the heat reservoir is to induce decay from $|A_2\rangle$ to $|m_s = \pm 1\rangle$. The decay rates are $\Gamma_{-1} = 2\pi \times 4.3$ MHz (from $|A_2\rangle$ to $|m_s = -1\rangle$) and $\Gamma_{+1} = 2\pi \times 8.5$ MHz (from $|A_2\rangle$ to $|m_s = +1\rangle$), as shown in Fig. 1(b). Moreover, the orbital dephasing of level $|A_2\rangle$ cannot be ignored [24], where the dephasing rate is $\Gamma_d = 2\pi \times 8.8$ MHz. All the decoherence rates mentioned here are selected from measurements in the recent experiment [9]. The dynamics of the Λ system is governed by

$$\partial_t\rho(t) = \hat{\mathcal{L}}_0\rho(t) + \Gamma_d\hat{\mathcal{D}}[L_d]\rho(t), \qquad (12)$$

where

$$
\begin{aligned}
\hat{\mathcal{L}}_0\rho(t) = &-\frac{i}{\hbar}[H_0(t), \rho] \\
&+ \sum_{\alpha=0,+1} \Gamma_\alpha\{(N_\alpha + 1)\hat{\mathcal{D}}[L_\alpha](\rho) + N_\alpha\hat{\mathcal{D}}[L_\alpha^\dagger](\rho)\}
\end{aligned}
$$

and $\hat{\mathcal{D}}[L_\alpha](\rho) = L_\alpha(t)\rho L_\alpha^\dagger(t) - \frac{1}{2}\{L_\alpha^\dagger(t)L_\alpha(t), \rho\}$. For the decay form $|A_2\rangle$, the Lindblad operators can be expressed as $L_{\pm 1} = |m_s = \pm 1\rangle\langle A_2|$ and $L_d = |A_2\rangle\langle A_2|$ for the orbital dephasing. By $N_\alpha = [\exp(\hbar\omega_{2\to\alpha}/kT) - 1]^{-1}$ we denote the mean excitation numbers. In the following discussion, we choose $\hat{\mathcal{L}}_0$ as the reference Liouvillian, and the dephasing is the key obstacle to the performance of the protocol.

A. The adiabatic trajectory

In this subsection, we present the control protocol where the quantum state transfers along the adiabatic trajectory given by the instantaneous steady state of $\hat{\mathcal{L}}_0(t)$. We parameterize the instantaneous steady state of $\hat{\mathcal{L}}_0(t)$ via the generalized Bloch vector $\{r_k\}_{k=1}^8$. The density matrix of the three-level system can be written as

$$\rho(t) = \frac{1}{3}\left(I + \sqrt{3}\sum_{k=1}^8 r_k(t)T_k\right), \qquad (13)$$

where I is a 3×3 identity matrix and T_k denotes the regular Gellmann matrix. These $\{T_k\}$ span all traceless Hermitian matrices of the Lie algebra su(3). If $\Gamma_{+1} = \Gamma_{-1} \equiv \Gamma$ and $N_{+1} = N_{-1} \equiv N$, the components of the Bloch vector corresponding to the instantaneous steady state of $\hat{\mathcal{L}}_0(t)$ are

$$r_2 = \sqrt{3}N\Gamma\Omega_p/z, \qquad (14a)$$

$$r_3 = \sqrt{3}[(3N^2 + 2N)\Gamma^2 + \Omega_s^2]/(2z), \qquad (14b)$$

$$r_4 = -\sqrt{3}\Omega_p\Omega_s/z, \qquad (14c)$$

$$r_7 = -\sqrt{3}N\Gamma\Omega_s/z, \qquad (14d)$$

$$r_8 = -[(3N^2 + 2N)\Gamma^2 + 2\Omega_p^2 - \Omega_s^2]/(2z), \qquad (14e)$$

with $z = (3N + 1)\Omega^2 + N\Gamma^2(3N + 2)^2$ and the other components zeros. The details for obtaining the instantaneous steady state can be found in Appendix C. Correspondingly, the dynamical invariants can be expressed by the Bloch vector according to the MIE scheme [see Eq. (8)]

$$\hat{\mathcal{I}}(t) = \Omega_I|\rho_0\rangle\rangle\langle\langle I|, \qquad (15)$$

where Ω_I is an arbitrary nonzero constant and $\langle\langle I|$ is the left vector corresponding to a 3×3 identity matrix.

Assume that the total Liouvillian reads

$$\hat{\mathcal{L}} = \hat{\mathcal{L}}_c + \Gamma_d\hat{\mathcal{D}}[L_d]. \qquad (16)$$

The control Liouvillian has the same form as Eq. (12),

$$
\begin{aligned}
\hat{\mathcal{L}}_c\rho(t) = &-i[H_c(t), \rho] \\
&+ \sum_{\alpha=\pm 1} \Gamma_\alpha\{(N_\alpha^i + 1)\hat{\mathcal{D}}[L_\alpha](\rho) + N_\alpha^i\hat{\mathcal{D}}[L_\alpha^\dagger](\rho)\},
\end{aligned}
\qquad (17)
$$

where the Hamiltonian is

$$H_c(t) = \frac{\hbar}{2}\begin{pmatrix} 0 & \Omega_p^i(t) & i\,\Omega_c^i(t) \\ \Omega_p^i(t) & 0 & \Omega_s^i(t) \\ -i\,\Omega_c^i(t) & \Omega_s^i(t) & 0 \end{pmatrix}. \qquad (18)$$

Here we also assume that the mean excitation numbers $N_{\pm 1}^i$ are tunable independently, which can be achieved by properly engineering the temperature of the environment [25] or shifting the energy difference between $|A_2\rangle$ and $|m_s = \pm 1\rangle$. Substituting Eqs. (15) and (17) into Eq. (2), we can determine all the control parameters in the control Liouvillian $\hat{\mathcal{L}}_c$. The analytical expressions for these control parameters are presented in Appendix D. Alternatively, these control parameters can be obtained numerically, especially for more complex situations such as $\Gamma_{-1} \neq \Gamma_{+1}$. Taking Eqs. (11) and (14) into the analytical expressions, we obtain the control parameters for the adiabatic trajectory with a time independent Ω:

$$\Omega_s^i = \Omega\sin[\theta(t)], \qquad \Omega_p^i = \Omega\cos[\theta(t)], \qquad \Omega_c^i = \partial_t\theta(t),$$

$$N_{-1}^i = N, \qquad N_{+1}^i = N.$$

These control parameters are exactly the parameters obtained in the transitionless quantum driving scheme of closed systems for the STIRAP [6].

Despite the MIE scheme and the transitionless driving scheme of closed systems providing similar control protocols for an adiabatic trajectory, their essences are quite different. The two schemes give similar control protocols only if $\Omega = \sqrt{\Omega_s^2(t) + \Omega_p^2(t)}$ is time independent. This can be illustrated by the spectrum decomposition of the instantaneous steady state of $\hat{\mathcal{L}}_0$. The eigenvalues of ρ_0 are

$$p_1 = \frac{1}{z}[(2N+1)(3N+2)N\Gamma^2 + 2N\Omega^2 - N\Gamma\sqrt{(3N+2)^2\Gamma^2 + 4\Omega^2}],$$

$$p_2 = \frac{1}{z}[(2N+1)(3N+2)N\Gamma^2 + 2N\Omega^2 + N\Gamma\sqrt{(3N+2)^2\Gamma^2 + 4\Omega^2}],$$

$$p_3 = \frac{N+1}{z}[(3N+2)N\Gamma^2 + \Omega^2],$$

with $z = (3N+1)\Omega^2 + N\Gamma^2(3N+2)^2$, which denote the populations on corresponding eigenstates. If Ω is constant, the population on every eigenstate is invariant, so that a unitary evolution is enough to transfer the quantum state into the target steady state. But if Ω is time dependent, the incoherent controls are required for the STIRAP process along the adiabatic trajectory because of time-varying purity of the quantum state.

Figures 2(a) and 2(b) show the control fields and the corresponding populations for the open Λ system at room temperature (300 K). The corresponding mean excitation number is $N = 1.9 \times 10^{-33}$. The boundary conditions of $\theta(t)$ are set to be $\theta(0) = 0$ and $\theta(\tau) = \pi/2$. We choose the simplest STIRAP pulses, i.e., $\theta(t) = \pi t/(2\tau)$, where τ is the pulse length. The numerical results of the control fields show that, for nonadiabatic state transfer along the adiabatic trajectory, the control protocol is completely the same as the protocol given by the transitionless quantum driving method [6]. This illustrates that the transitionless driving method [26,27] will present a better transfer efficiency than any other scheme [9,28], if Ω is set to be constant. As shown in Fig. 2(b), the quantum state is transferred into the target state with a perfect final population. In Fig. 2(c), we plot the final population not on $|m_s = +1\rangle$ [denoted by $\log_{10}(1 - P_3)$ with $P_3 = \langle m_s = +1|\rho(\tau)|m_s = +1\rangle$] as a function of the pulse length τ for both the adiabatic scheme (the red dotted and blue dot-dash lines) and the MIE scheme (green dash and black solid lines). Compared to the adiabatic scheme, our scheme can transfer the population into $|m_s = +1\rangle$ with a transfer efficiency very close to 1 (at least 10^{-6}; see the figure). Since $|A_2\rangle$ is unoccupied, our protocol is immune to the orbital dephasing encountered in earlier proposals.

In practical applications, the initial-to-final state coupling Ω_c^i can be implemented in some but not all systems, e.g., because of selection rules due to symmetry of the
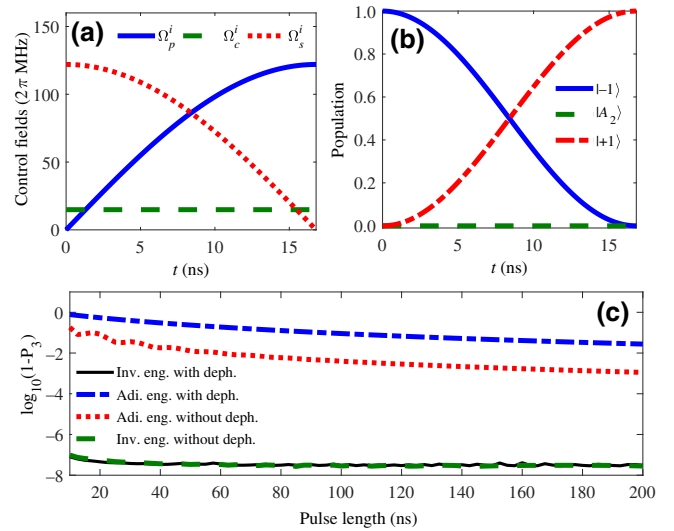

FIG. 2. (a) The control fields and (b) the populations on $|m_s = -1\rangle$ (blue solid line), $|A_2\rangle$ (green dash line), and $|+1\rangle$ (red dot-dash line) as a function of time for pulse length $\tau = 16.8$ ns. (c) The final population on states except $|m_s = +1\rangle$ as a function of the pulse length τ for $\Omega = 2\pi \times 122$ MHz, $\Gamma_{-1} = 2\pi \times 4.3$ MHz, $\Gamma_{+1} = 2\pi \times 8.4$ MHz, $\Gamma_d = 2\pi \times 8.8$ MHz, and $N = 1.9 \times 10^{-33}$.

states or the necessary phase of the term. In nitrogen-vacancy electronic spins, this additional coupling was implemented mechanically via a strain field in the recent experiment [29,30]. The strain field to drive N-V spins is based on the sensitive response of the N-V spin states to strain in the diamond host lattice. For uniaxial strain applied transverse to the N-V axis, the transverse strain field couples the electronic spin states $|m_s = -1\rangle$ and $|m_s = +1\rangle$. To realize such a strain field for efficient coherent driving, a mechanical resonator is required in the form of a singly clamped, single-crystalline diamond cantilever, in which the N-V center is directly embedded [30]. The cantilever is actuated at its mechanical resonance frequency $\omega_m = 2\pi \times 6.84$ MHz. Thus, for resonance driving, the external magnetic field satisfies $B_{\text{N-}V} = 2.42$ G. And the corresponding Rabi frequency is characterized by $\Omega_c = \gamma_T x_c / x_{\text{ZPF}}$, where γ_T is the transverse single-phonon strain-coupling strength, x_c and x_{ZPF} are the cantilever's zero-point fluctuation and peak amplitude, respectively (with $\gamma_T \sim 2\pi \times 0.08$ MHz and $x_{\text{ZPF}} \sim 7.7 \times 10^{-15}$ m). Therefore, we can tune the cantilever's amplitude x_c to adjust the Rabi frequency of the strain field.

B. The trajectory without initial-to-final state couplings

In experiment, an initial-to-final state coupling induced by the strain field $\Omega_c^i(t)$ can be realized in an artificial structure but not in real atoms via dipole-dipole coupling due to the selection rule. The pure-state inverse engineering

scheme solves this by providing alternative shortcuts that do not directly couple levels $|m_s = -1\rangle$ and $|m_s = +1\rangle$ [19]. In the following, we show that the MIE scheme has the same quality via selecting a proper trajectory of the quantum state. Also, this particular trajectory can be obtained only by solving differential equations about the components of the Bloch vector, but not to design a complex transformation of the entire trajectory as done in the STA schemes of closed quantum systems. More importantly, our protocol is robust to the decay and dephasing noise at the same time.

We consider the case where the Stocks pulse and the pumping pulse resonantly excite both $|m_s = 0\rangle$ and $|m_s = +1\rangle$ to the excited-state spin singlet $|^1E\rangle$, as shown in Fig. 1(c). The singlet-ground ($|m_s = 0\rangle \rightarrow |^1E\rangle$) splitting is about 89 THz. The decay from the singlet state to the ground states is a spin nonpreserving nonradiative decay. The corresponding decay rates depend on the static magnetic field $\mathbf{B}_{N\text{-}V}$ with an angle η with respect to the N-V defect axis. It has been shown that the decay rates are approximatively equal for $\eta = \pi/10$, and have been measured in the lab with the results $\Gamma_0 \approx \Gamma_{+1} = 2\pi \times 1.5$ MHz [31]. Moreover, due to spin nonpreserving decay, the effective rate of the population excitation from $|m_s = 0\rangle$ to $|^1E\rangle$ is much lower than the decay rate from $|^1E\rangle$ to $|m_s = 0\rangle$, while the effective rate from $|m_s = +1\rangle$ to $|^1E\rangle$ is almost equal to its corresponding decay rate. Consequently, the $|m_s = +1\rangle - |^1E\rangle$ and $|m_s = 0\rangle - |^1E\rangle$ subsystems can be seen as coupling to two different thermal reservoirs [32]. It has also been shown in Ref. [32] that tuning the strength of $\mathbf{B}_{N\text{-}V}$ can effectively engineer temperatures of the thermal reservoirs.

In order to cancel the initial-to-final state coupling, the control field $\Omega_c^i(t)$ must be zero at any point in time. A direct method is to modify the trajectory of the quantum state. Here, we consider the case where the decay rates are equal. As illustrated in the analytical expressions of the control parameters (see Appendix D), $\Omega_c^i(t)$ can be written as a function of the Bloch vector and its time derivative $\{r_i, \partial_t r_i\}_{i=1}^8$. What we may do is to force $r_4(t)$ to vary in a proper way such that $\Omega_c^i(t) = 0$. To be specific, we consider the requirement $\Omega_c^i(t) = 0$ as a restriction to solve the differential equation for $r_4(t)$, keeping other components of the Bloch vector unchanged. This finally leads to a proper trajectory that cancels the initial-to-final state coupling.

By choosing a trajectory according to the instantaneous steady state of $\hat{\mathcal{L}}_0$ (see Appendix E), we plot the control parameters and the populations as a function of time in Fig. 3. We note that the additional coupling $\Omega_c^i(t)$ is eliminated in the engineering process [green solid line in Fig. 3(a)], and the population is transferred from $|m_s = 0\rangle$ into the target state $|m_s = +1\rangle$ with high transfer efficiency, as shown in Fig. 3(c). In addition, the excitation numbers of the reservoirs need to be engineered accordingly [see Fig. 3(b)].
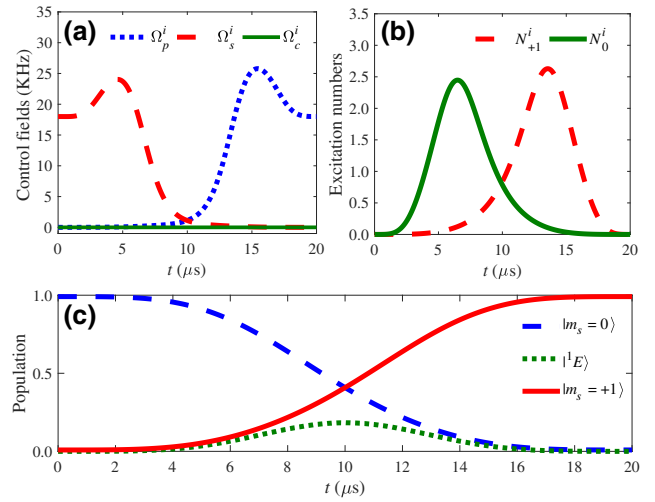

FIG. 3. (a) The control fields, (b) the mean excitation numbers, and (c) the populations on states $|m_s = 0\rangle$ (blue lines), $|^1E\rangle$ (green lines), and $|m_s = +1\rangle$ (red lines) as a function of time for $\Omega = 18.1$ KHz, $\Gamma = 2\pi \times 1.5$ MHz, $\Gamma_d = 2\pi \times 8.8$ MHz, and $N = 6.55 \times 10^{-7}$. The pulse length is $\tau = 20\ \mu$s.

Although Fig. 3 presents positive main excitation numbers, these main excitation numbers may still be negative at some points in time. In experiment, we may restrict the main excitation numbers to be within the regime $N_0^i, N_{+1}^i \geq 6.55 \times 10^{-7}$, which corresponds to $T_{\text{cutoff}} \approx 300$ K. In Fig. 4(a), we plot the final population that is not on $|m_s = +1\rangle$ as a function of the pulse length τ for the control field $\Omega = 154$ KHz. Both dynamical processes with (red dash line) and without (blue solid line) the dephasing noise are considered in Fig. 4. As we see, the MIE scheme fails to transfer the population into $|m_s = +1\rangle$ for short pulse lengths due to the cutoff on the main excited number N_{+1}^i. But it performs good when prolonging the pulse length, and the final population on $|m_s = +1\rangle$ asymptotically approaches a predicted value given by the instantaneous steady state of $\hat{\mathcal{L}}_0(\tau)$. On the other hand, since the coherence between $|^1E\rangle$ and $|m_s = 0\rangle$ ($|m_s = +1\rangle$) in our designed trajectory is negligible, the orbital dephasing noise of $|^1E\rangle$ will not affect the state transfer process. The numerical result confirms our analysis; see the blue solid and red dashed lines in Fig. 4(a). We also present the results given by the superadiabatic scheme [30] with (green dotted line) and without (black dash-dot line) dephasing noise. As a pure-state STA scheme, the superadiabatic scheme needs to keep states as pure states. When $|^1E\rangle$ is populated, strong coherence between the excited and ground states is required, so that pure-state STA schemes are sensitive to dephasing noise. Therefore, the MIE scheme is more robust to orbital dephasing noise than the STA schemes of closed quantum systems.

We also plot the population on all states except $|m_s = +1\rangle$ (blue solid line) as a function of the control field Ω
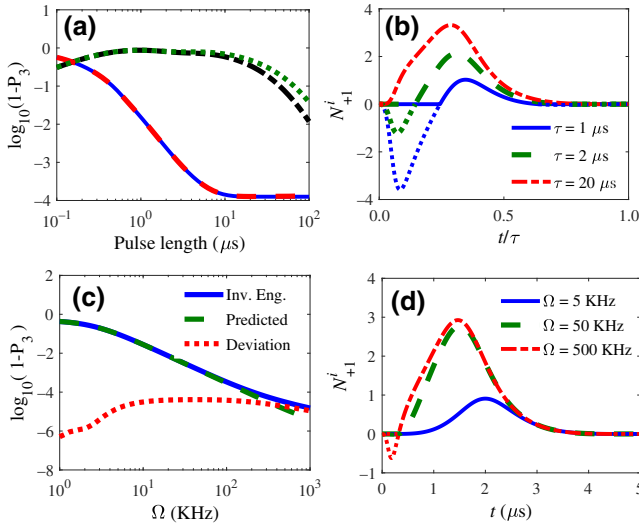
FIG. 4. The final population not on $|m_s = +1\rangle$ (red lines) as a function of (a) the pulse length τ for $\Omega = 154$ KHz and (c) the control fields Ω for $\tau = 5$ μs. The main excitation number N^i_{+1} as a function of time with (b) different pulse lengths for $\Omega = 154$ KHz and (d) different control fields for $\tau = 5$ μs. The other parameters in the master equation are chosen as $\Gamma = 2\pi \times 1.5$ MHz, $\Gamma_d = 2\pi \times 8.8$ MHz, and $N = 6.55 \times 10^{-7}$.

with a pulse length $\tau = 5$ μs in Fig. 4(c). As expected, the final population on $|m_s = +1\rangle$ increases with the control field. The population not on $|m_s = +1\rangle$ given by the steady state $\rho_0(\tau)$ is also plotted; see the green dashed line. We find that the final population for inverse engineering cannot reach the predicted value due to the main excitation number cutoff; see Fig. 4(d). As illustrated by the red dotted line in Fig. 4(c), the worst deviation of the final population is no more than 10^{-4}. Therefore, although the final population deviates from the predicted value, we can still obtain a satisfactory transfer efficiency in the regime of a strong control field.

IV. COMPARISON WITH THE PURE-STATE INVERSE ENGINEERING SCHEME

A. Pure-state engineering

In this section, we compare the MIE scheme to the pure-state inverse engineering (PIE) scheme. Firstly, we show that the STA scheme of open quantum systems includes the PIE scheme. To inversely engineering a pure state, the dynamical invariants $I(t)$ of closed systems are needed [18], which satisfy

$$i\partial_t I(t) = [H(t), I(t)]$$

with $H(t)$ the Hamiltonian. The general solution of closed systems can be written as

$$|\Psi(t)\rangle = \sum_n c_n \exp[i\alpha_n(t)]|\psi_n(t)\rangle, \quad (19)$$

where the c_n are time-independent amplitudes, the $|\psi_n(t)\rangle$ are orthonormal eigenvectors of the invariant $I(t)$, and the $\alpha_n(t)$ are the Lewis-Riesenfeld phases. According to the general solution, Eq. (19), we can write the time-dependent unitary evolution operator U as

$$U(t) = \sum_n \exp[i\alpha_n(t)]|\psi_n(t)\rangle\langle\psi_n(0)|,$$

which obeys

$$i\partial_t U(t) = H(t)U(t).$$

Thus, we obtain the formal expression of the Hamiltonian as

$$H(t) = \sum_n [i|\partial_t \psi_n(t)\rangle\langle\psi_n(t)| - \partial_t \alpha_n(t)|\psi_n(t)\rangle\langle\psi_n(t)|]. \quad (20)$$

If we impose $[H(0), I(0)] = [H(\tau), I(\tau)] = 0$, the eigenstates coincide and then a state transfer from a initial eigenstate of the Hamiltonian to the final one is guaranteed.

For applying the STA scheme of open quantum systems to a pure-state engineering task, we can formulate the dynamical invariant superoperator $\hat{\mathcal{I}}$ by the eigenstates of a closed system's dynamical invariant. The time-dependent eigenstates of $\hat{\mathcal{I}}$ are chosen as

$$|\Psi_{mn}\rangle\rangle = |\psi_m\rangle \otimes |\psi_n^*\rangle, \quad (21)$$

which corresponds to the time-independent eigenvalues λ_{mn}. Substituting $\{|\Psi_{mn}\rangle\rangle\}$ into Eq. (5), the control Liouvillian superoperator can be obtained with arbitrary phases $\eta_{mn}(t)$. Thus, $\hat{\mathcal{L}}_c(t)$ transfers the quantum state from $|\psi_n(0)\rangle$ to $|\psi_n(\tau)\rangle$ along with $|\Psi_{nn}(t)\rangle\rangle$. According to Eq. (5), the control Liouvillian can be written as

$$\hat{\mathcal{L}}_c(t) = \sum_{mn} (|\partial_t \Psi_{mn}\rangle\rangle\langle\langle\Psi_{mn}| + \partial_t\eta_{mn}|\Psi_{mn}\rangle\rangle\langle\langle\Psi_{mn}|).$$

By considering Eq. (21), we obtain

$$\hat{\mathcal{L}}_c(t) = \sum_{mn} [|\partial_t \psi_m\rangle\langle\psi_m| \otimes (|\psi_n\rangle\langle\psi_n|)^* \\ + |\psi_m\rangle\langle\psi_m| \otimes (\partial_t|\psi_n\rangle\langle\psi_n|)^* \\ + \partial_t\eta_{mn}|\Psi_{mn}\rangle\rangle\langle\langle\Psi_{mn}|].$$

Since $\{|\psi_m\rangle\}$ is a complete set of the Hilbert space, we have

$$\hat{\mathcal{L}}_c(t) = -i\left[i\sum_{mn}\partial_t\eta_{mn}|\Psi_{mn}\rangle\rangle\langle\langle\Psi_{mn}| + \left(\sum_m i|\partial_t\psi_m\rangle\langle\psi_m|\right) \\ \otimes I - I \otimes \left(\sum_n i\partial_t|\psi_n\rangle\langle\psi_n|\right)^*\right],$$

where I is an identity matrix. If the phase satisfies $\eta_{mn} = i(\alpha_m - \alpha_n)$, we obtain

$$\hat{\mathcal{L}}_c(t) = -i\left[\left(i\sum_m |\partial_t\psi_m\rangle\langle\psi_m| - \partial_t\alpha_m|\partial_t\psi_m\rangle\langle\psi_m|\right)\otimes I\right.$$
$$\left. - I\otimes\left(i\sum_n \partial_t|\psi_n\rangle\langle\psi_n| - \partial_t\alpha_n|\partial_t\psi_n\rangle\langle\psi_n|\right)^*\right].$$

Considering the map from the superoperator to operators, $A\otimes B^*|\rho\rangle\rangle \mapsto A\rho B^\dagger$ for arbitrary operators A and B, we immediately have

$$\hat{\mathcal{L}}_c(t)|\rho(t)\rangle\rangle = -i[H(t), \rho(t)], \qquad (22)$$

where $H(t)$ is just the Hamiltonian involved in the PIE scheme as shown in Eq. (20). Therefore, the STA scheme of open quantum systems includes the PIE scheme.

In the following, we take the STIRAP as an example to show that the STA scheme gives the same control protocol as the PIE scheme. Following the steps in Ref. [19], the eigenstates of dynamical invariant are given by

$$|\psi_0\rangle = \begin{pmatrix} \cos\gamma\,\cos\beta \\ -i\sin\gamma \\ -\cos\gamma\,\sin\beta \end{pmatrix},$$

$$|\psi_\pm\rangle = \frac{\sqrt{2}}{2}\begin{pmatrix} \sin\gamma\,\cos\beta \pm i\sin\beta \\ i\cos\gamma \\ -\sin\gamma\,\sin\beta \pm i\cos\beta \end{pmatrix}.$$

Thus, we can formulate the eigenstate of the dynamical invariant superoperator according to Eq. (21). Substituting Eq. (21) into Eq. (5), we obtain the control Liouvillian $\hat{\mathcal{L}}_c$ as a function of β, γ, and phases η_{mn}. Comparing η_{mn} with the Lewis-Riesenfeld phases α_n, we immediately find that $\eta_{mn} = i(\alpha_m - \alpha_n)$. Thus, we have $\eta_{nn} = 0$, $\eta_{+-} = -\eta_{-+} \equiv \eta_1$, $\eta_{+0} = -\eta_{0+} \equiv \eta_2$, and $\eta_{0-} = -\eta_{-0} \equiv \eta_3$. The control Liouvillian can be expanded by SU(3) generators [T_i, the regular Gellmann matrices; see Eqs. (C3)], i.e.,

$$\hat{\mathcal{L}}_c(t) = \sum_{i,j=1}^{9} c_{ij} T_i \otimes T_j^*,$$

where T_9 is a 3×3 identity matrix and the c_{ij} are time-dependent expanding coefficients, which can be determined by

$$c_{ij} = \text{Tr}[\hat{\mathcal{L}}(t)T_i \otimes T_j^*].$$

Moreover, if the phase η_k $(k=1,2,3)$ satisfies the relations $\eta_2 = \eta_1/2$ and $\eta_3 = -\eta_1/2$, we obtain the coefficient matrix

$$c = \frac{i}{2}\begin{pmatrix} 0 & 0 & 0 & 0 & 0 & 0 & 0 & 0 & -2\partial_t\gamma\cos\beta - \eta_1\cos\gamma\sin\beta \\ 0 & 0 & 0 & 0 & 0 & 0 & 0 & 0 & 0 \\ 0 & 0 & 0 & 0 & 0 & 0 & 0 & 0 & 0 \\ 0 & 0 & 0 & 0 & 0 & 0 & 0 & 0 & 0 \\ 0 & 0 & 0 & 0 & 0 & 0 & 0 & 0 & 2\partial_t\beta - \eta_1\sin\gamma \\ 0 & 0 & 0 & 0 & 0 & 0 & 0 & 0 & 2\partial_t\gamma\sin\beta - \eta_1\cos\beta\cos\gamma \\ 0 & 0 & 0 & 0 & 0 & 0 & 0 & 0 & 0 \\ 0 & 0 & 0 & 0 & 0 & 0 & 0 & 0 & 0 \\ 2\partial_t\gamma\cos\beta + \eta_1\cos\gamma\sin\beta & 0 & 0 & 0 & -2\partial_t\beta + \eta_1\sin\gamma & -2\partial_t\gamma\sin\beta + \eta_1\cos\beta\cos\gamma & 0 & 0 & 0 \end{pmatrix}.$$

In other words, the control Liouvillian reads

$$\hat{\mathcal{L}}_c(t) = -i[(2\partial_t\gamma\cos\beta + \eta_1\cos\gamma\sin\beta)(T_1\otimes T_9^* - T_9\otimes T_1^*)$$
$$+ (2\partial_t\beta - \eta_1\sin\gamma)(T_5\otimes T_9^* - T_9\otimes T_5^*)$$
$$+ (\eta_1\cos\beta\cos\gamma - 2\partial_t\gamma\sin\beta)(T_6\otimes T_9^* - T_9\otimes T_6^*)].$$

Thus, the control Liouvillian can be transformed as

$$\hat{\mathcal{L}}_c(t)|\rho(t)\rangle\rangle \mapsto -i[H(t), \rho(t)] \qquad (23)$$

with $H(t) = \Omega_p/2\, T_1 + \Omega_c/2\, T_5 + \Omega_s/2\, T_6$, in which the control fields are

$$\Omega_p = \eta_1\cos\gamma\sin\beta + 2\partial_t\gamma\cos\beta,$$
$$\Omega_c = 2\partial_t\beta - \eta_1\sin\gamma,$$
$$\Omega_s = \eta_1\cos\beta\cos\gamma - 2\partial_t\gamma\sin\beta.$$

In order to cancel initial-to-final state couplings, the phase η_1 has to be selected as $\eta_1 = 2\partial_t\beta/\sin\gamma$. Taking η_1 into the above equations, we immediately obtain the same control protocol given in Ref. [19], i.e.,

$$\Omega_p = 2\partial_t\beta\cot\gamma\sin\beta + 2\partial_t\gamma\cos\beta, \qquad (24a)$$

$$\Omega_s = 2\partial_t\beta\cot\gamma\cos\beta - 2\partial_t\gamma\sin\beta, \qquad (24b)$$

$$\Omega_c = 0. \qquad (24c)$$

Therefore, the STA scheme of open quantum systems is equivalent to the PIE scheme if the control task is to transfer pure states with a pure-state trajectory.

B. Pure-state engineering with mixed-state trajectories

The MIE scheme provides more feasible control protocols than the PIE scheme, because the trajectory does not have to be a pure-state trajectory. As illustrated by the STRIAP of open quantum systems, the robustness to the dephasing noise attributes to the mixed-state trajectory with weak coherence between the energy levels. In this subsection, we show that the MIE scheme overcomes the difficulties of the PIE scheme. As shown in Eqs. (24), $|^1E\rangle$ needs to be populated to avoid infinitely large $\Omega_{p,s}$. The strengths of the control fields satisfy $\Omega_{p,s} \propto 1/\sqrt{P_2}$, where $P_2 = \sin^2\gamma$ is the population on $|^1E\rangle$. For the control protocol given by the MIE scheme, reasonable and feasible $\Omega_{p,s}$ are needed instead of infinitely large control fields, which is illustrated in Fig. 5(a).

For the control protocol given by the PIE scheme, the parameters in Eqs. (24) are chosen as $\gamma = (\gamma_m - \gamma_0)\sin^3(\pi t/\tau) + \gamma_0$ with constants γ_m and γ_0; $\beta = \pi/2\sin[\pi t/(2\tau)]$. For the mixed-state protocol, we set an analogous trajectory with $r_3 = -\sqrt{3}(\sin^2\gamma - \cos^2\beta\cos^2\gamma)/2$, $r_8 = (3\sin^2\gamma + 3\cos^2\beta\cos^2\gamma - 2)/2$. Since the mixed-state protocol does not need the population on $|^1E\rangle$, we set $\gamma_0 = 0$ in the mixed-state trajectory. The other components of the Bloch vector are $r_2 = -\sin^2\xi\cos\beta$ and $r_7 = \sin^2\xi\sin\beta$ with $\xi = \xi_0\sin^2(2\pi t/\tau)$; r_4 is used to cancel the initial-final state coupling, which is determined by the equation $\Omega_c^i(r_4) = 0$.

In Figs. 5(a) and 5(b), we plot the control field Ω_p and the population on $|^1E\rangle$ as a function of the dimensionless time t/τ. The red dashed lines are the results given by the mixed-state protocol, and the green dot-dash and blue solid lines are the numerical results given by the pure-state protocol with $\gamma_0 = 0.1$ and $\gamma_0 = 0.01$, respectively. As shown in Fig. 5(a), the mixed-state protocol only requires a finite strength of the control field Ω_p^i, even if the population on $|^1E\rangle$ is zero. But, for the PIE scheme, the strength of Ω_p tends to infinity when the population on $|^1E\rangle$ goes to zero
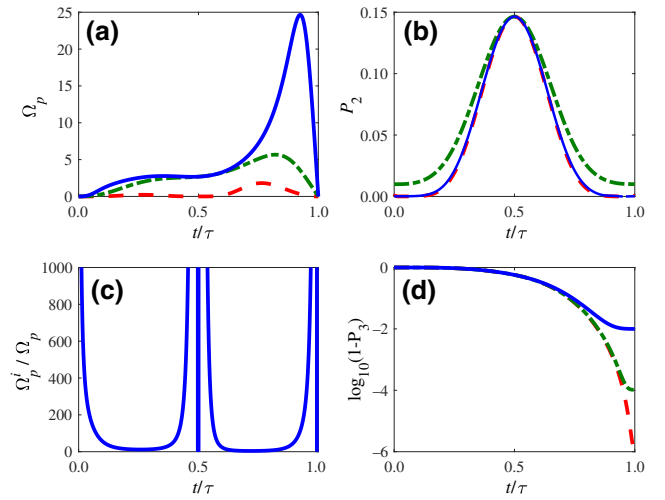

FIG. 5.   (a) The control field Ω_p, (b) the population on $|^1E\rangle$, (c) the ratio of the control field strengths between the mixed-state and the pure-state inverse engineering schemes, and (d) the population out of $|+1\rangle$ versus the dimensionless time t/τ for the mixed-state trajectory (red dash lines) and the pure state trajectory with $\gamma_0 = 0.1$ (green dot-dash lines) and $\gamma_0 = 0.01$ (blue solid lines). The decay rate is chosen as $\Gamma = 10/\tau$.

at $t/\tau = 1$. The finite control field strength is the contribution from designable r_2 and r_7. For $t/\tau = 1$, the final state satisfies $r_3 = 0$, $r_8 = -1$, and $r_4 = 0$, and the time derivatives of these components of the general Bloch vector are zeros. Then, we can obtain the control field Ω_p^i as a function of r_2 and r_7 from Eq. (D1), which reads

$$\Omega_p^i = -\frac{2\sqrt{3}\partial_t r_7 r_2 - \sqrt{3}\partial_t r_2 r_7 + 2\sqrt{3}\Gamma r_2 r_7}{2r_2(-r_2^2 + r_7^2 + 3)}. \qquad (25)$$

This equation illustrates that, even if $|^1E\rangle$ is unpopulated, we can still obtain a finite control field by selecting a proper relation between r_2 and r_7. Substituting the concrete parameterized r_2 and r_7 into Eq. (25), we finally obtain $\Omega_p^i(\tau) = 0$. To illustrate this clearly, we further plot the ratio between the control fields for the mixed-state protocol $\Omega_p^i(t)$ and the pure-state protocol $\Omega_p(t)$ with $\gamma_0 = 0.01$ in Fig. 5(c). When $t/\tau \to 0$ and $t/\tau \to 1$ (the minimal population on $|^1E\rangle$ for the pure-state protocol), the ratio goes to infinity, which verifies that the mixed-state protocol does not require an extremely strong control field in the control process. As shown in Fig. 5(d), the MIE scheme also presents a better transfer efficiency than the pure-state inverse engineering scheme.

V. CONCLUSION

To achieve feasible control of open quantum systems with high accuracy, high controllability, and high speed, we propose a fast and robust control scheme. After presenting the STA based on dynamical invariants of open

quantum systems, we apply STA of open quantum systems to accelerate the adiabatic steady process. As a result, with the same form as the reference Liouvillian, the control Liouvillian can drive the open quantum system from an initial steady state into a target steady state along a designed trajectory with desired fidelity and pulse length. We highlight the high controllability of the trajectory, which leads to robustness of control protocols to some particular noises and eliminates untunable control manners.

Our scheme opens several promising avenues for further developments. Theoretically, it would be interesting to explore possible speed limits and trade-off relations for the open quantum systems [33,34]. Experimentally, due to the feasible of the MIE protocol, the present protocol can be realized in various systems, such as cavity quantum electrodynamical systems [35], superconducting circuits [27], nitrogen-vacancy centers [26], and spin chains [36].

APPENDIX A: THE GENERAL SOLUTION OF EQ. (1)

The dynamical invariants $\hat{\mathcal{I}}(t)$ are defined as superoperators that satisfy the dynamical equation

$$\partial_t \hat{\mathcal{I}}(t) - [\hat{\mathcal{L}}_c(t), \hat{\mathcal{I}}(t)] = 0, \tag{A1}$$

where $\hat{\mathcal{L}}(t)$ is the control Liouvillian superoperator. Generally speaking, the superoperator $\hat{\mathcal{I}}(t)$ is non-Hermitian. We can introduce a right basis $\{|D_\alpha^{(i)}\rangle\rangle\}$ and left basis $\{\langle\langle E_\alpha^{(i)}|\}$ in Hilbert-Schmidt space based on the Jordan canonical form. The left and right bases always satisfy

$$\hat{\mathcal{I}}|D_\alpha^{(i)}\rangle\rangle = \lambda_\alpha |D_\alpha^{(i)}\rangle\rangle + |D_\alpha^{(i-1)}\rangle\rangle, \tag{A2a}$$

$$\langle\langle E_\alpha^{(i)}|\hat{\mathcal{I}} = \lambda_\alpha \langle\langle E_\alpha^{(i)}| + \langle\langle E_\alpha^{(i+1)}|, \tag{A2b}$$

where

$$|D_\alpha^{(-1)}\rangle\rangle \equiv 0, \tag{A3}$$

$$\langle\langle E_\alpha^{(n_\alpha)}| \equiv 0, \tag{A4}$$

with $i = 0, 1, \ldots, n_\alpha - 1$ (n_α is the dimension of block α). Here we assume that all the eigenvalues are nondegenerate, i.e., $\lambda_\alpha \neq \lambda_\beta$ for all $\alpha \neq \beta$. Moreover, the left and right bases satisfy the orthonormality condition

$$\langle\langle E_\alpha^{(i)}|D_\beta^{(j)}\rangle\rangle = \delta_{\alpha\beta}\delta_{ij}$$

The right and left bases $|D_\alpha^{(0)}\rangle\rangle$ and $\langle\langle E_\alpha^{(n_\alpha-1)}|$ are the right and left eigenvectors of $\hat{\mathcal{I}}(t)$ with the eigenvalue λ_α. Taking the first derivative of Eq. (A2a) with respect to time,

we have

$$\partial_t \hat{\mathcal{I}}|D_\alpha^{(i)}\rangle\rangle + \hat{\mathcal{I}}|\partial_t D_\alpha^{(i)}\rangle\rangle$$
$$= \partial_t \lambda_\alpha |D_\alpha^{(i)}\rangle\rangle + \lambda_\alpha |\partial_t D_\alpha^{(i)}\rangle\rangle + |\partial_t D_\alpha^{(i-1)}\rangle\rangle. \tag{A5}$$

Multiplying the above equation by $\langle\langle E_\beta^{(j)}|$ yields

$$\langle\langle E_\beta^{(j)}|\partial_t \hat{\mathcal{I}}|D_\alpha^{(i)}\rangle\rangle$$
$$= \partial_t \lambda_\alpha \delta_{\alpha\beta}\delta_{ij} + (\lambda_\alpha - \lambda_\beta)\langle\langle E_\beta^{(j)}|\partial_t D_\alpha^{(i)}\rangle\rangle$$
$$+ \langle\langle E_\beta^{(j)}|\partial_t D_\alpha^{(i-1)}\rangle\rangle - \langle\langle E_\beta^{(j+1)}|\partial_t D_\alpha^{(i)}\rangle\rangle. \tag{A6}$$

Substituting Eq. (A1) into the last equation, we obtain

$$\partial_t \lambda_\alpha \delta_{\alpha\beta}\delta_{ij} = (\lambda_\alpha - \lambda_\beta)\langle\langle E_\beta^{(j)}|\hat{O}|D_\alpha^{(i)}\rangle\rangle$$
$$+ \langle\langle E_\beta^{(j)}|\hat{O}|D_\alpha^{(i-1)}\rangle\rangle - \langle\langle E_\beta^{(j+1)}|\hat{O}|D_\alpha^{(i)}\rangle\rangle, \tag{A7}$$

where $\hat{O} \equiv \hat{\mathcal{L}}_c - \partial_t$.

For $\alpha \neq \beta$, the above equation yields

$$(\lambda_\alpha - \lambda_\beta)\langle\langle E_\beta^{(j)}|\hat{O}|D_\alpha^{(i)}\rangle\rangle + \langle\langle E_\beta^{(j)}|\hat{O}|D_\alpha^{(i-1)}\rangle\rangle$$
$$- \langle\langle E_\beta^{(j+1)}|\hat{O}|D_\alpha^{(i)}\rangle\rangle = 0. \tag{A8}$$

In the following, we illustrate that $\langle\langle E_\beta^{(j)}|\hat{O}|D_\alpha^{(i)}\rangle\rangle = 0$ for all i, j. Firstly, we note that the above equation is a recurrence equation about the i and j indexes. Setting $i = 0$ and $j = n_\beta - 1$, we obtain

$$\langle\langle E_\beta^{(n_\beta-1)}|\hat{O}|D_\alpha^{(0)}\rangle\rangle = 0, \tag{A9}$$

where Eqs. (A3) and (A4) are used. Then, using the recurrence equation (A8) again and considering $i = 1$ and $j = n_\beta - 1$, we obtain

$$(\lambda_\alpha - \lambda_\beta)\langle\langle E_\beta^{(n_\beta-1)}|\hat{O}|D_\alpha^{(1)}\rangle\rangle + \langle\langle E_\beta^{(n_\beta-1)}|\hat{O}|D_\alpha^{(0)}\rangle\rangle = 0.$$

Substituting Eq. (A9) into the above equation, we have

$$\langle\langle E_\beta^{(n_\beta-1)}|\hat{O}|D_\alpha^{(1)}\rangle\rangle = 0. \tag{A10}$$

Repeating this procedure and checking every index $i = 1, \ldots, n_\alpha - 1$, we conclude that the follow relations hold:

$$\langle\langle E_\beta^{(n_\beta-1)}|\hat{O}|D_\alpha^{(i)}\rangle\rangle = 0 \quad \text{for all } i = 0, \ldots, n_\alpha - 1. \tag{A11}$$

Secondly, we check $\langle\langle E_\beta^{(j)}|\hat{O}|D_\alpha^{(0)}\rangle\rangle$ by the same procedure as before. Setting $j = n_\beta - 2$, Eq. (A8) becomes

$$(\lambda_\alpha - \lambda_\beta)\langle\langle E_\beta^{(n_\beta-2)}|\hat{O}|D_\alpha^{(0)}\rangle\rangle + \langle\langle E_\beta^{(n_\beta-2)}|\hat{O}|D_\alpha^{(-1)}\rangle\rangle$$
$$- \langle\langle E_\beta^{(n_\beta-1)}|\hat{O}|D_\alpha^{(0)}\rangle\rangle = 0.$$

Because of the relation in Eqs. (A3) and (A9), we immediately have

$$\langle\langle E_\beta^{(n_\beta-2)}|\hat{O}|D_\alpha^{(0)}\rangle\rangle = 0.$$

Thus, reducing the index j step by step and checking all terms by Eq. (A8), we conclude that

$$\langle\langle E_\beta^{(j)}|\hat{O}|D_\alpha^{(0)}\rangle\rangle = 0. \tag{A12}$$

Equipped with Eqs. (A11) and (A12), we check the other i and j indexes by the recurrence equation. For instance, setting $i=1$ and $j=n_\beta-2$, we have

$$(\lambda_\alpha-\lambda_\beta)\langle\langle E_\beta^{(n_\beta-2)}|\hat{O}|D_\alpha^{(1)}\rangle\rangle + \langle\langle E_\beta^{(n_\beta-2)}|\hat{O}|D_\alpha^{(0)}\rangle\rangle$$
$$- \langle\langle E_\beta^{(n_\beta-1)}|\hat{O}|D_\alpha^{(1)}\rangle\rangle = 0.$$

We obtain

$$\langle\langle E_\beta^{(n_\beta-2)}|\hat{O}|D_\alpha^{(1)}\rangle\rangle = 0, \tag{A13}$$

using Eqs. (A11) and (A12). As a result, when all of the i and j indexes are iterated, we conclude that

$$\langle\langle E_\beta^{(j)}|\hat{O}|D_\alpha^{(i)}\rangle\rangle = 0 \quad \text{for all } i,j \tag{A14}$$

for $\lambda_\alpha \neq \lambda_\beta$ for all $\alpha \neq \beta$.

In the $\alpha=\beta$ case, Eq. (A7) can be written as

$$\partial_t\lambda_\alpha\delta_{ij} = \langle\langle E_\alpha^{(j)}|\hat{O}|D_\alpha^{(i-1)}\rangle\rangle - \langle\langle E_\alpha^{(j+1)}|\hat{O}|D_\alpha^{(i)}\rangle\rangle.$$

Therefore, we can obtain the dynamical equation of the eigenvalues by taking the sum over all i and j indexes of the Jordan block α,

$$\partial_t\lambda_\alpha = \frac{1}{n_\alpha}\sum_{i,j=0}^{n_\alpha-1}(\langle\langle E_\alpha^{(j)}|\hat{O}|D_\alpha^{(i-1)}\rangle\rangle - \langle\langle E_\alpha^{(j+1)}|\hat{O}|D_\alpha^{(i)}\rangle\rangle).$$

If $i \neq j$, we find that

$$\langle\langle E_\alpha^{(j)}|\hat{O}|D_\alpha^{(i-1)}\rangle\rangle = \langle\langle E_\alpha^{(j+1)}|\hat{O}|D_\alpha^{(i)}\rangle\rangle.$$

Thus, we can write the dynamical equation of eigenvalues as

$$\partial_t\lambda_\alpha = \frac{1}{n_\alpha}\left(\sum_{i=0}^{n_\alpha-1}\langle\langle E_\alpha^{(i)}|\hat{O}|D_\alpha^{(i-1)}\rangle\rangle - \sum_{j=0}^{n_\alpha-1}\langle\langle E_\alpha^{(j+1)}|\hat{O}|D_\alpha^{(j)}\rangle\rangle\right).$$

Replacing the index j by $k=j+1$, we obtain

$$\partial_t\lambda_\alpha = \frac{1}{n_\alpha}\left(\sum_{i=0}^{n_\alpha-1}\langle\langle E_\alpha^{(i)}|\hat{O}|D_\alpha^{(i-1)}\rangle\rangle - \sum_{k=1}^{n_\alpha}\langle\langle E_\alpha^{(k)}|\hat{O}|D_\alpha^{(k-1)}\rangle\rangle\right)$$
$$= \frac{1}{n_\alpha}(\langle\langle E_\alpha^{(0)}|\hat{O}|D_\alpha^{(-1)}\rangle\rangle - \langle\langle E_\alpha^{(n_\alpha)}|\hat{O}|D_\alpha^{(n_\alpha-1)}\rangle\rangle).$$

Then, by considering Eqs. (A3) and (A4), we finally obtain

$$\partial_t\lambda_\alpha = 0, \tag{A15}$$

which implies that the dynamical invariants indeed have time-independent eigenvalues.

Let us now consider the solution of the master equation with the Liouvillian $\hat{\mathcal{L}}_c(t)$, i.e.,

$$\partial_t|\rho(t)\rangle\rangle = \hat{\mathcal{L}}_c(t)|\rho(t)\rangle\rangle. \tag{A16}$$

We expand the density matrix vector by the left basis vectors of the dynamical invariant $\hat{\mathcal{I}}(t)$,

$$|\rho(t)\rangle\rangle = \sum_{\alpha=0}^{m-1} c_\alpha(t)|\Phi_\alpha(t)\rangle\rangle \tag{A17}$$

with

$$|\Phi_\alpha(t)\rangle\rangle = \sum_{i=0}^{n_\alpha-1} b_i^\alpha(t)|D_\alpha^{(i)}(t)\rangle\rangle, \tag{A18}$$

where m is the number of Jordan blocks. Inserting Eq. (A17) into Eq. (A16), we obtain

$$\sum_{\alpha=0}^{m-1}\partial_t c_\alpha(t)|\Phi_\alpha(t)\rangle\rangle + \sum_{\alpha=0}^{m-1}c_\alpha(t)\partial_t|\Phi_\alpha(t)\rangle\rangle$$
$$= \sum_{\alpha=0}^{m-1}c_\alpha(t)\hat{\mathcal{L}}_c(t)|\Phi_\alpha(t)\rangle\rangle. \tag{A19}$$

Here we define a left vector $\langle\langle\Psi_\beta(t)|$ of the Jordan block β, which satisfies $\langle\langle\Psi_\beta(t)|\Phi_\alpha(t)\rangle\rangle = \delta_{\alpha\beta}$. This left vector can be expanded by the left basis vectors of the Jordan block β, i.e., $\langle\langle\Psi_\beta(t)| = \sum_{j=0}^{n_\beta-1}a_j^\beta(t)\langle\langle E_\beta^{(j)}(t)|$. Projecting Eq. (A19) into $\langle\langle\Psi_\beta(t)|$, we obtain

$$\partial_t c_\beta(t) = \sum_{\alpha=0}^{m-1}c_\alpha(t)\langle\langle\Psi_\beta(t)|\hat{O}(t)|\Phi_\alpha(t)\rangle\rangle \tag{A20}$$

with

$$\langle\langle\Psi_\beta(t)|\hat{O}(t)|\Phi_\alpha(t)\rangle\rangle = \sum_{i,j}a_j^\beta(t)b_i^\alpha(t)\langle\langle E_\beta^{(j)}|\hat{O}|D_\alpha^{(i)}\rangle\rangle.$$

By making use of Eq. (A14), we have

$$\partial_t c_\beta(t) = c_\beta(t)\langle\langle\Psi_\beta(t)|\hat{O}(t)|\Phi_\beta(t)\rangle\rangle. \tag{A21}$$

This results in a formal solution of the density matrix vector

$$|\rho(t)\rangle\rangle = \sum_{\alpha=0}^{m-1}c_\alpha(0)|\tilde{\Phi}_\alpha(t)\rangle\rangle \tag{A22}$$

with "dynamical modes" $|\tilde{\Phi}_\alpha(t)\rangle\rangle = \exp[\eta_\alpha(t)]|\Phi_\alpha(t)\rangle\rangle$, where the phases are defined as

$$\eta_\alpha(t) = \int_0^t d\tau \langle\langle\Psi_\alpha(\tau)|\hat{O}(\tau)|\Phi_\alpha(\tau)\rangle\rangle. \qquad (A23)$$

In fact, we do not obtain a complete solution of the master equation (A16), since the coefficients in $|\phi_\alpha(t)\rangle\rangle$ have not been determined. This will be an interesting open question for further investigation. But the formal solution in Eq. (A22) is enough to establish the shortcuts to adiabaticity of open quantum systems, since the adiabatic theorem of open quantum systems just requires that the transitions between different Jordan blocks are forbidden [10]. Putting undetermined coefficients in $|\phi_\alpha(t)\rangle\rangle$ aside, we only need to ensure that the quantum state is in the same Jordan block of $\hat{\mathcal{L}}_c(t)$ at the beginning and end of control process.

APPENDIX B: COMPARISON WITH THE TRANSITIONLESS DRIVING SCHEME OF OPEN QUANTUM SYSTEMS

In the following, we present a proof that our scheme is as general as, and in some cases beyond, Vacanti's method [15].

For the reference Liouvillian superoperator $\hat{\mathcal{L}}_0(t)$, it is always possible to find a similarity transformation $C(t)$ such that $\hat{\mathcal{L}}_0(t)$ is written in the canonical Jordan form

$$\hat{\mathcal{L}}_J(t) = C^{-1}(t)\hat{\mathcal{L}}_0(t)C(t) = \mathrm{diag}[J_1(t),\ldots,J_N(t)], \quad (B1)$$

where $J_\alpha(t)$ represents the Jordan block (of dimension n_α) corresponding to the eigenvalue $\zeta_\alpha(t)$ of $\hat{\mathcal{L}}_0(t)$. The number N of Jordan blocks is equal to the number of linearly independent eigenvectors of $\hat{\mathcal{L}}_0(t)$ and the similarity transformation is given by

$$C(t) = \sum_{\alpha=1}^N \sum_{i=1}^{n_\alpha} |D_\alpha^{(i)}(t)\rangle\rangle\langle\langle\sigma_\alpha^{(i)}|,$$

where $\{|D_\alpha^{(i)}(t)\rangle\rangle\}$ is a right instantaneous quasieigenbasis of $\hat{\mathcal{L}}_0(t)$ associated with the eigenvalues $\{\zeta_\alpha(t)\}$ that satisfies

$$\hat{\mathcal{L}}_0|D_\alpha^{(i)}\rangle\rangle = \zeta_\alpha|D_\alpha^{(i)}\rangle\rangle + |D_\alpha^{(i-1)}\rangle\rangle.$$

Furthermore, $\{|\sigma_\alpha^{(i)}\rangle\rangle\}$ is a set of time-independent bases that is used to calculate the matrix form of $\hat{\mathcal{L}}_0(t)$.

Here we construct a dynamical invariant superoperator $\hat{\mathcal{I}}(t)$ that has the same Jordan blocks structure. In other words, $\hat{\mathcal{I}}(t)$ can be diagonal by the same similarity transformation $C(t)$, i.e.,

$$\hat{\mathcal{I}}_J = C^{-1}(t)\hat{\mathcal{I}}(t)C(t) = \mathrm{diag}[I_1,\ldots,I_N], \qquad (B2)$$

where I_α is the Jordan block (of dimension n_α) corresponding to the eigenvalue λ_α of $\hat{\mathcal{I}}(t)$. The eigenvalues $\{\lambda_\alpha\}$ are

time independent. In fact, choosing a dynamical invariant with the same Jordan block structure is equivalent to choosing the trajectory of the mixed-state inverse engineering as the adiabatic trajectory. Therefore, $\hat{\mathcal{L}}_0(t)$ and $\hat{\mathcal{I}}(t)$ share common quasieigenvectors $|D_\alpha^{(i)}(t)\rangle\rangle$, i.e.,

$$\hat{\mathcal{I}}|D_\alpha^{(i)}\rangle\rangle = \lambda_\alpha|D_\alpha^{(i)}\rangle\rangle + |D_\alpha^{(i-1)}\rangle\rangle.$$

The dynamical invariants $\hat{\mathcal{I}}(t)$ satisfy the dynamical equation (A1). Following Vacanti's method, the control Liouvillian superoperator can be written as $\hat{\mathcal{L}}(t) = \hat{\mathcal{L}}_0(t) + \hat{\mathcal{L}}_c(t)$, where $\hat{\mathcal{L}}_c(t)$ is the counterdiabatic superoperator. Substituting Eq. (B2) into Eq. (A1), we obtain

$$\partial_t(C\hat{\mathcal{I}}_J C^{-1}) = [C\hat{\mathcal{L}}_J C^{-1} + \hat{\mathcal{L}}_c, C\hat{\mathcal{I}}_J C^{-1}], \qquad (B3)$$

where Eq. (B1) has been used. Considering that $\hat{\mathcal{I}}_J$ is time independent and taking the same similarity transformation $C(t)$ as in the above equation, we obtain

$$[C^{-1}\partial_t C, \hat{\mathcal{I}}_J] = [\hat{\mathcal{L}}_J, \hat{\mathcal{I}}_J] + [C^{-1}\hat{\mathcal{L}}_c C, \hat{\mathcal{I}}_J], \qquad (B4)$$

where we have used the fact that $C^{-1}\partial_t C = -\partial_t C^{-1} C$. Since $\hat{\mathcal{I}}(t)$ and $\hat{\mathcal{L}}_0(t)$ have the same Jordan block structure, we have $[\hat{\mathcal{L}}_J, \hat{\mathcal{I}}_J] = 0$. It is not difficult to see that, if $\hat{\mathcal{L}}'_c \equiv C^{-1}\hat{\mathcal{L}}_c C = C^{-1}\partial_t C$, Eq. (B4) holds. We expand $\hat{\mathcal{L}}'_c$ by the bases $\{|\sigma_\alpha^{(i)}\rangle\rangle\}$, and separate it into two parts, $\hat{\mathcal{L}}'_c = \hat{\mathcal{L}}'_J + \hat{\mathcal{L}}'_{\mathrm{nd}}$, where

$$\hat{\mathcal{L}}'_J = \sum_{\alpha,i,j} C_\alpha^{i,j} |\sigma_\alpha^{(i)}\rangle\rangle\langle\langle\sigma_\alpha^{(j)}|,$$

$$\hat{\mathcal{L}}'_{\mathrm{nd}} = \sum_{\alpha\neq\beta,i,j} C_{\alpha,\beta}^{i,j} |\sigma_\alpha^{(i)}\rangle\rangle\langle\langle\sigma_\beta^{(j)}|,$$

with $C_{\alpha,\beta}^{i,j} = \langle\langle\sigma_\alpha^{(j)}|C^{-1}\partial_t C|\sigma_\beta^{(i)}\rangle\rangle$. The superoperator $\hat{\mathcal{L}}'_{\mathrm{nd}}$ contains all of non-diagonal blocks of $\hat{\mathcal{L}}'_c$ which is used to forbid transitions from J_α to J_β. Therefore, the counterdiabatic superoperator that is really required for STA is

$$\hat{\mathcal{L}}_{\mathrm{tqd}}(t) = C(t)\hat{\mathcal{L}}'_{\mathrm{nd}}(t)C^{-1}(t). \qquad (B5)$$

The subscript tqd indicates that $\hat{\mathcal{L}}_{\mathrm{tqd}}$ is the counterdiabatic superoperator used in the transitionless quantum driving scheme for open quantum systems. Comparing Eq. (B5) with Eq. (15) of Ref. [15], we immediately find that $\hat{\mathcal{L}}_{\mathrm{tqd}}(t)$ is the very counterdiabatic superoperator given by Vacanti and his coauthors [15].

The above simple proof illustrates that, if the trajectory of the general STA based on the invariant theory of open quantum systems is chosen as the adiabatic trajectory,

our method is coincident with the transitionless quantum driving method proposed in Ref. [15]. However, the adiabatic trajectory is not the only choice for the trajectories in our scheme. There are many trajectories that can be used to inversely engineer the open quantum system. As shown by the example in Sec. III B, proper trajectories can always produce reasonable and applicable control protocols, which helps us to overcome the difficulties met in the control of microscopic or/and mesoscopic systems. Hence, mixed-state inverse engineering is more general than the transitionless quantum driving method of open quantum systems proposed by Vacanti *et al.* [15].

The main difficulty with Vacanti's method is how to realize the counterdiabatic superoperator in practical control. The MIE scheme solves this problem by selecting proper trajectories. According to the symmetry of open quantum systems, we can flexibly choose the form of the control Liouvillian, making the proposal widely applicable in the control of open quantum systems.

APPENDIX C: THE INSTANTANEOUS STEADY STATE OF $\hat{\mathcal{L}}_0(t)$

We use the "bra-ket" notation for the superoperator to rewrite the master equation (12), and reshape the density matrix into a 1×9 complex vector. The density matrix vector can be written as

$$|\rho\rangle\rangle = (\rho_{-1-1}, \rho_{-12}, \rho_{-11}, \rho_{2-1}, \rho_{22}, \rho_{21}, \rho_{1-1}, \rho_{12}, \rho_{11})^\top$$

with $\rho_{ij} = \langle i|\hat{\rho}|j\rangle$. In order to present an analytic result, we assume that $\Gamma_{-1} = \Gamma_{+1} \equiv \Gamma$ and $\omega_{2\to-1} = \omega_{2\to+1} \equiv \omega_0$. At room temperature ($T = 300$ K), the mean excitation number is $N = 1.9 \times 10^{-33}$. For a practice application, we choose the instantaneous steady state of the reference Liouvillian $\hat{\mathcal{L}}_0$ as the trajectory of inverse engineering; in this case the dephasing is the key obstacle to the performance of the protocol. The reference Liouvillian superoperator $\hat{\mathcal{L}}_0$ can be expressed as a 9×9 matrix,

$$\hat{\mathcal{L}}_0 = \hbar\Gamma \begin{pmatrix} -2N & i\Omega_p/\Gamma & 0 & -i\Omega_p/\Gamma & 2(N+1) & 0 & 0 & 0 & 0 \\ i\Omega_p/\Gamma & -(3N+2) & i\Omega_s/\Gamma & 0 & -i\Omega_p/\Gamma & 0 & 0 & 0 & 0 \\ 0 & i\Omega_s/\Gamma & -2N & 0 & 0 & -i\Omega_p/\Gamma & 0 & 0 & 0 \\ -i\Omega_p/\Gamma & 0 & 0 & -(3N+2) & i\Omega_p/\Gamma & 0 & -i\Omega_s/\Gamma & 0 & 0 \\ 2N & -i\Omega_p/\Gamma & 0 & i\Omega_p/\Gamma & -4(N+1) & i\Omega_s/\Gamma & 0 & -i\Omega_s/\Gamma & 2N \\ 0 & 0 & -i\Omega_p/\Gamma & 0 & i\Omega_s/\Gamma & -(3N+2) & 0 & 0 & -i\Omega_s/\Gamma \\ 0 & 0 & 0 & -i\Omega_s/\Gamma & 0 & 0 & -2N & i\Omega_p/\Gamma & 0 \\ 0 & 0 & 0 & 0 & -i\Omega_s/\Gamma & 0 & i\Omega_p/\Gamma & -(3N+2) & i\Omega_s/\Gamma \\ 0 & 0 & 0 & 0 & 2(N+1) & -i\Omega_s/\Gamma & 0 & i\Omega_s/\Gamma & -2N \end{pmatrix}.$$

The steady state is obtained immediately by considering $\hat{\mathcal{L}}_0|\rho_0\rangle\rangle = 0$,

$$|\rho_0\rangle\rangle = \frac{1}{z} \begin{pmatrix} (3N^2 + 2N)(N+1)\Gamma^2 + N\Omega^2 + \Omega_p{}^2 \\ -iN\Gamma\Omega_p \\ -\Omega_p\Omega_s \\ iN\Gamma\Omega_p \\ N^2(3N+2)\Gamma^2 + N\Omega^2 \\ iN\Gamma\Omega_s \\ -\Omega_p\Omega_s \\ -iN\Gamma\Omega_s \\ (3N^2 + 2N)(N+1)\Gamma^2 + N\Omega^2 + \Omega_s{}^2 \end{pmatrix}$$
(C1)

with normalized factor

$$z = (3N+1)\Omega^2 + N\Gamma^2(3N+2)^2.$$

For $N = 0$, the instantaneous steady state is the dark state of Hamiltonian (10), i.e., $|\rho_0\rangle\rangle = (\cos^2\theta, 0, \sin\theta\cos\theta, 0, 0, 0, \sin\theta\cos\theta, 0, \sin^2\theta)^\top$.

We parameterize the adiabatic trajectory given by the instantaneous steady state of $\hat{\mathcal{L}}_0$ via the generalized Bloch vector $\{r_k\}_{k=1}^8$, which expands the density matrix of the three-level system as

$$\rho(t) = \frac{1}{3}\left(I + \sqrt{3}\sum_{k=1}^{8} r_k(t)T_k\right), \quad \text{(C2)}$$

where I is a 3×3 identity matrix and the T_k denote the regular Gellmann matrices

$$T_1 = \begin{pmatrix} 0 & 1 & 0 \\ 1 & 0 & 0 \\ 0 & 0 & 0 \end{pmatrix}, \qquad T_2 = \begin{pmatrix} 0 & -i & 0 \\ i & 0 & 0 \\ 0 & 0 & 0 \end{pmatrix}, \quad \text{(C3a)}$$

$$T_3 = \begin{pmatrix} 1 & 0 & 0 \\ 0 & -1 & 0 \\ 0 & 0 & 0 \end{pmatrix}, \qquad T_4 = \begin{pmatrix} 0 & 0 & 1 \\ 0 & 0 & 0 \\ 1 & 0 & 0 \end{pmatrix}, \quad \text{(C3b)}$$

$$T_5 = \begin{pmatrix} 0 & 0 & -i \\ 0 & 0 & 0 \\ i & 0 & 0 \end{pmatrix}, \qquad T_6 = \begin{pmatrix} 0 & 0 & 0 \\ 0 & 0 & 1 \\ 0 & 1 & 0 \end{pmatrix}, \quad \text{(C3c)}$$

$$T_7 = \begin{pmatrix} 0 & 0 & 0 \\ 0 & 0 & -i \\ 0 & i & 0 \end{pmatrix}, \qquad T_8 = \frac{1}{\sqrt{3}} \begin{pmatrix} 1 & 0 & 0 \\ 0 & 1 & 0 \\ 0 & 0 & -2 \end{pmatrix}.$$

$$\text{(C3d)}$$

These $\{T_\mu\}$ span all traceless Hermitian matrices of the Lie algebra su(3). Thus, the Bloch vectors corresponding to the instantaneous steady state, Eq. (C1), are

$$r_2 = \sqrt{3} N \Gamma \Omega_p / z, \tag{C4a}$$

$$r_3 = \sqrt{3} [(3N^2 + 2N)\Gamma^2 + \Omega_s{}^2]/(2z), \tag{C4b}$$

$$r_4 = -\sqrt{3} \Omega_p \Omega_s / z, \tag{C4c}$$

$$r_7 = -\sqrt{3} N \Gamma \Omega_s / z, \tag{C4d}$$

$$r_8 = -[(3N^2 + 2N)\Gamma^2 + 2\Omega_p{}^2 - \Omega_s{}^2]/(2z), \tag{C4e}$$

and the other components are zeros. Correspondingly, the dynamical invariants can be parameterized by the Bloch vector according to our proposal [see Eq. (8)],

$$\hat{\mathcal{I}}(t) = \frac{\sqrt{3}}{3} \Omega_I \begin{pmatrix} \left(r_3 + \frac{\sqrt{3}r_8}{3}\right) + \frac{\sqrt{3}}{3} & 0 & 0 & 0 & \left(r_3 + \frac{\sqrt{3}r_8}{3}\right) + \frac{\sqrt{3}}{3} & 0 & 0 & 0 & \left(r_3 + \frac{\sqrt{3}r_8}{3}\right) + \frac{\sqrt{3}}{3} \\ ir_2 & 0 & 0 & 0 & ir_2 & 0 & 0 & 0 & ir_2 \\ r_4 & 0 & 0 & 0 & r_4 & 0 & 0 & 0 & r_4 \\ -ir_2 & 0 & 0 & 0 & -ir_2 & 0 & 0 & 0 & -ir_2 \\ \frac{\sqrt{3}}{3} - \left(r_3 - \frac{\sqrt{3}r_8}{3}\right) & 0 & 0 & 0 & \frac{\sqrt{3}}{3} - \left(r_3 - \frac{\sqrt{3}r_8}{3}\right) & 0 & 0 & 0 & \frac{\sqrt{3}}{3} - \left(r_3 - \frac{\sqrt{3}r_8}{3}\right) \\ ir_7 & 0 & 0 & 0 & ir_7 & 0 & 0 & 0 & ir_7 \\ r_4 & 0 & 0 & 0 & r_4 & 0 & 0 & 0 & r_4 \\ -ir_7 & 0 & 0 & 0 & -ir_7 & 0 & 0 & 0 & -ir_7 \\ \frac{\sqrt{3}}{3} - \frac{2\sqrt{3}r_8}{3} & 0 & 0 & 0 & \frac{\sqrt{3}}{3} - \frac{2\sqrt{3}r_8}{3} & 0 & 0 & 0 & \frac{\sqrt{3}}{3} - \frac{2\sqrt{3}r_8}{3} \end{pmatrix}, \tag{C5}$$

where Ω_I is an arbitrary nonzero constant.

APPENDIX D: THE CONTROL PARAMETERS IN THE CONTROL LIOUVILLIAN

Considering the dynamical equation of the dynamical invariants, Eq. (A1), we can determine all the control parameters in the control Liouvillian $\hat{\mathcal{L}}_c$,

$$\Omega_s^i = n_s/d, \quad \Omega_p^i = n_p/d, \quad \Omega_c^i = n_c/d, \quad N_{-1}^i = n_{-1}/d, \quad N_{+1}^i = n_{+1}/d, \tag{D1}$$

in which

$$d = 2\sqrt{3} r_4{}^4 C_2 + 4\sqrt{3} r_2{}^4 C_1 + r_2{}^2 [12 r_8 (r_4{}^2 + r_7{}^2) + 12\sqrt{3}(r_3{}^2 + r_8{}^2)C_1]$$
$$+ r_4{}^2 (6 r_7{}^2 C_2 - 8\sqrt{3} r_3 C_1 C_2) + 8 r_3{}^2 C_2 C_1{}^2 + 4\sqrt{3} r_3 r_7{}^2 (r_2{}^2 - 2 r_7{}^2) - 8 r_2 r_4 r_7 (\sqrt{3} r_7{}^2 + 3 C_2 C_4) + 8\sqrt{3} r_2{}^3 r_4 r_7$$
$$+ 12 r_3 r_7{}^2 [r_3 - (\sqrt{3} - 2) r_8][(2\sqrt{3} + 3) r_8 + \sqrt{3} r_3],$$

$$n_s = 2\sqrt{3} \partial_t r_2 [r_4{}^2 (r_7{}^2 - C_1 C_2) + 2 r_2{}^2 r_3 C_1 + r_2 r_4 r_7 (C_2 + 4 r_3) + 2 r_3 C_2 (2 r_7{}^2 + C_1{}^2)]$$
$$+ \sqrt{3} \partial_t r_3 \{-2 r_2{}^3 C_1 + 2 r_2 [-C_1{}^2 C_2 - 2 r_7{}^2 (C_2 + r_3)] - r_4 r_7 (4 r_2{}^2 + r_4{}^2 - r_7{}^2 + 2\sqrt{3} r_8 C_1)\}$$
$$+ \partial_t r_4 [-r_7 (4 r_3 C_1{}^2 - 6 r_4{}^2 C_3) - 4\sqrt{3} r_3 r_7 (r_2{}^2 + 2 r_7{}^2) - 2\sqrt{3} r_2 r_4 (2 C_1 C_2 + 3 r_7{}^2)]$$
$$+ 2\sqrt{3} \partial_t r_7 [2 r_3 r_4 C_1 C_2 - r_4{}^3 C_2 - (2\sqrt{3} r_2 r_8 - r_4 r_7)(r_2 r_4 + 2 r_3 r_7)]$$

$$+ \partial_t r_8 \{r_2[2C_1C_2^2 + 2r_4^2C_2 + 2r_7^2(r_3 + C_1)] + 2r_2^3C_2 + r_4r_7(4C_2^2 + 2r_2^2 + r_4^2 + r_7^2 + 2\sqrt{3}r_8C_1)\}$$

$$+ \Gamma r_2^2[14r_4r_7 + 2r_4r_7(C_3 + 3\sqrt{3}r_3)] - r_7^3[2r_4 + 2r_4(C_3 - 6\sqrt{3}r_3)]$$

$$- \Gamma r_7[r_4^3(8C_3 - 4) - r_4(4\sqrt{3}r_3^3 - 44r_3^2r_8 + 4r_3^2 + 4\sqrt{3}r_3r_8^2 + 16\sqrt{3}r_3r_8 - 12r_8^3 - 12r_8^2)]$$

$$- \Gamma r_2^3(4\sqrt{3}r_8 - 8r_3 + 4r_8C_2) + \Gamma r_2r_7^2(16r_3 + 4\sqrt{3}r_8 + 4r_8C_2)$$

$$+ \Gamma r_2r_4^2[8\sqrt{3}r_7^2 + (2 - 6\sqrt{3}r_3 + 14r_8)C_2] - \Gamma r_2C_1C_2(4\sqrt{3}r_8 - 8r_3 + 4r_8C_2),$$

$$n_p = \partial_t r_2[6r_4^3C_2 - r_4(12r_3C_1C_2 - 6\sqrt{3}r_7^2C_3) + 6r_2r_7(r_4^2 + \sqrt{3}C_1C_3) + 6r_2^2r_4C_1]$$

$$+ \partial_t r_3\left[3r_4^2r_7C_2 - 6r_2^2r_7C_1 - 3r_2r_4[r_4^2 + 3r_7^2 - 2C_1(r_3 + C_2)] + 6r_7 - C_1\left(r_3C_2 - \frac{r_7^2}{2}\right)\right]$$

$$+ 6\partial_t r_4\{-2C_1r_2^3 - 3r_4r_7r_2^2 + [-2\sqrt{3}r_8r_4^2 - C_1(4r_3^2 + r_7^2)]r_2 - 4r_3r_4r_7C_2\}$$

$$+ \partial_t r_7[r_2^2(-12C_1C_2 + 6r_4^2) - 24r_3^2C_1C_2 + 12r_3r_4^2C_2 + 12r_3r_7^2C_1 + 6r_2r_4r_7(3C_1 - 2r_3)]$$

$$+ \partial_t r_8\{\sqrt{3}r_4^2r_7C_2 - 4\sqrt{3}r_2^2r_7C_2 - \sqrt{3}r_2r_4[2(r_3 + C_2)^2 - 5r_7^2] - \sqrt{3}r_2r_4(2r_2^2 - r_4^2)\}$$

$$+ \partial_t r_8[-7\sqrt{3}r_3r_7(2r_3^2 - r_7^2) + 2\sqrt{3}r_3r_8(r_2r_4 - 3r_7r_8) - 3r_7r_8(4r_3 - r_7)(4r_3 + r_7)]$$

$$+ \Gamma r_2[2r_7^2(-2r_3 + 5C_1 + 7\sqrt{3}) - 4\sqrt{3}(r_8 + 1)(4r_3^2 + C_1C_2) + 36r_3r_4(r_3^2 + r_8^2)]$$

$$+ \Gamma\{-r_7^3(-4r_8 - 10C_4 + 2\sqrt{3}C_2C_3) + r_2^2[2r_7C_2^2 - 12r_7(3r_8 - 2r_4^2) + 2r_7C_2(2r_3 + \sqrt{3})]\}$$

$$+ \Gamma\{r_2^3[18r_4C_1 - 2\sqrt{3}r_4(2r_8 + 1)] + 4\sqrt{3}(4r_8 + 1)r_2r_4^3\}$$

$$- \Gamma r_7\{r_4^2C_2(2\sqrt{3} - 30r_3 + 2\sqrt{3}r_8) - 4r_3[C_2(2r_8 - 5C_4) + r_3C_2(5C_3 - 2r_3) - \sqrt{3}r_8C_1C_2]\},$$

$$n_c = \partial_t r_2[6r_2r_4(r_7^2 + \sqrt{3}C_1C_4) + 12r_3r_7(r_4^2 + 2r_7^2) - 6r_2^2r_7C_1 + 12r_3r_7C_1^2]$$

$$+ \partial_t r_3\{r_4(6r_3C_1^2 + 3r_7^2C_2) - 3r_4^3C_1 - 6r_2^2r_4C_1 - r_2r_7[3r_4^2 + 9r_7^2 + 6C - 1(r_3 - C_1)]\}$$

$$+ \partial_t r_4[12r_3r_4^2C_1 - r_2^2(12C_1^2 + 18r_7^2) - 24r_3^2(C_1^2 + 2r_7^2) - 6\sqrt{3}r_2r_4r_7C_4]$$

$$+ \partial_t r_7\{6r_7[r_2(r_2r_4 - 2r_3r_7) - 2\sqrt{3}r_3r_4C_4] + 12r_2^3C_1 + 6r_2C_1(4r_3^2 + r_4^2)\}$$

$$+ \partial_t r_8\{(3r_8 + 3\sqrt{3}r_3)r_4^3 + [3r_7^2(r_8 + 3\sqrt{3}r_3) + 12r_2^2r_8 - 6r_3(r_8 + \sqrt{3}r_3)(r_3 - \sqrt{3}r_8)]r_4\}$$

$$+ \partial_t r_8[r_2r_7(6\sqrt{3}r_2^2 + 4\sqrt{3}r_3^2 + \sqrt{3}r_4^2 - 3\sqrt{3}r_7^2) + 6\frac{\sqrt{3}}{3}r_2r_7C_4(r_8 + 2C_3)]$$

$$+ \Gamma\{r_2^2[24r_4r_7^2 - 6r_4(r_8 - \sqrt{3}r_3)(\sqrt{3}r_3 - 5r_8 + 1)] - 6r_2^3r_7(r_3 + \sqrt{3}r_8 - \sqrt{3})\}$$

$$+ \Gamma(r_2\{(6C_2 + 6\sqrt{3})r_7^3 + [r_4^2(8\sqrt{3}C_4 + 4\sqrt{3}) + 4\sqrt{3}(\sqrt{3}C_1C_4 + 4r_3^2) + 4\sqrt{3}C_2^2C_1]r_7\})$$

$$+ \Gamma\{r_4r_7^2[6C_4 + \sqrt{3}C_4(18r_3 + 2\sqrt{3}r_8)] - 6r_4^3C_4(C_4 + 2) + 12r_3C_1C_4r_4(C_4 - 1)\},$$

$$n_{-1} = \partial_t r_2[6\sqrt{3}r_4r_7(C_1^2 - 3r_2^2 + r_4^2 + 2r_7^2) - 6\sqrt{3}r_2^3C_1 - \sqrt{3}r_2(6C_1^2C_2 - 12r_4^2C_1 + 12r_7^2C_2)]$$

$$+ \partial_t r_3\{-3\sqrt{3}r_2^2[(r_4^2 - r_7^2) + 6r_3C_1] - \sqrt{3}r_7^2[9r_3 + (\sqrt{3} + 2)r_8][r_3 - (\sqrt{3} - 2)r_8]\}$$

$$+ \partial_t r_3[3\sqrt{3}(3r_7^4 - r_4^4) - 6\sqrt{3}r_3C_2C_1^2 + 9r_4^2C_1C_3 - 24\sqrt{3}r_2r_3r_4r_7]$$

$$+ \partial_t r_4\{6\sqrt{3}r_7r_2(C_1^2 - 3r_4^2 + 2r_7^2 + r_2^2) + \sqrt{3}r_4[6C_1(r_4^2 - 2r_2^2) - 12r_3(C_1^2 + 2r_7^2)]\}$$

$$+ \partial_t r_7\{\sqrt{3}[6r_7(2\sqrt{3}r_8r_2^2 - \sqrt{3}r_4^2C_4) + 6r_2r_4(C_1^2 + r_2^2 + r_4^2 - 2r_7^2)]\}$$

$$+ \partial_t r_8\{-r_2^2[-r_2^2 + 3r_4^2 + 9r_7^2 + 6C_1(r_3 + C_2)] - 6r_3C_2C_1^2\}$$

$$+ \partial_t r_8\{3r_4^2(r_4^2 + 3r_7^2 - C_1^2) + 6r_7^4 - r_7^2[9r_3 + (\sqrt{3} + 2)r_8][r_3 - (\sqrt{3} - 2)r_8]$$

$$- 24\sqrt{3}r_2r_4r_7r_8\} + \Gamma\{\sqrt{3}r_2^4[2\sqrt{3}(2r_8 - 1) - 6C_1] - 24r_2r_4r_7[\sqrt{3}(r_2^2 - r_4^2) - \sqrt{3}C_4 + 2\sqrt{3}(r_3^2 - r_8^2)]\}$$

$$+ \Gamma(-r_2{}^2\{6C_1^2(3C_3 + 2r_8 - 1) + \sqrt{3}r_4{}^2[2\sqrt{3}(2r_8 - 1) - 18C_1] + 6\sqrt{3}r_7{}^2(C_2 + \sqrt{3})\})$$

$$+ \Gamma(12(1 - C_1)r_4{}^4 + \{18r_7{}^2(C_4 + 1) - 2\sqrt{3}C_1(4r_3 + C_2)[-2C_1 - \sqrt{3}(r_8 - 1)]\}r_4{}^2)$$

$$+ \Gamma\{12r_3C_2C_1^2 - 12r_7{}^4 + 18r_7{}^2[r_3 + (\sqrt{3} + 2)r_8][r_3 - (\sqrt{3} - 2)r_8]\}(1 - C_4),$$

$$\begin{aligned}
n_{+1} = {} & \partial_t r_2[6r_2(r_7{}^2 C_3 - r_4{}^2 C_4) - 2\sqrt{3}r_4 r_7(-2r_2{}^2 + 4r_3{}^2 + r_4{}^2 + r_7{}^2)] \\
& + \partial_t r_3\{(r_4{}^2 + r_7{}^2)[6r_3 r_8 + \sqrt{3}(r_4{}^2 - r_7{}^2)] + 2\sqrt{3}[r_4{}^2(r_2 + r_3)^2 - r_7{}^2(r_2 - r_3)^2]\} \\
& + \partial_t r_4[4\sqrt{3}(r_2{}^2 + 2r_3{}^2)r_4 C_1 - 4\sqrt{3}r_3 r_4(r_4{}^2 - 2r_7{}^2) - 2\sqrt{3}r_2 r_7(2r_2{}^2 + 4r_3{}^2 - 3r_4{}^2 + r_7{}^2)] \\
& + \partial_t r_7[-4\sqrt{3}r_2{}^2 r_7 C_2 - 4\sqrt{3}r_3 r_7(2r_4{}^2 - r_7{}^2 + 2r_3 C_2) - 2\sqrt{3}r_2 r_4(2r_2{}^2 + 4r_3{}^2 + r_4{}^2 - 3r_7{}^2)] \\
& + \partial_t r_8[4(r_2{}^2 + C_1 C_2)(r_2{}^2 + 2r_3{}^2) - (2r_3{}^2 + r_4{}^2 + r_7{}^2)(r_4{}^2 + r_7{}^2) + 8\sqrt{3}r_2 r_4 r_7 r_8 - 6\sqrt{3}r_3 r_8(r_4{}^2 - r_7{}^2)] \\
& + \Gamma[(2r_8 + 6\sqrt{3}r_3 + 2)r_7{}^4 + 4(r_2{}^4 - r_4{}^4)(1 - C_4)] \\
& + \Gamma\{-r_2{}^2[6r_4{}^2(C_4 + 1) + 2r_7{}^2(\sqrt{3}C_2 - 3) - 12(r_3{}^2 - r_8{}^2)(1 - C_4)]\} \\
& + \Gamma[4r_3 r_4{}^2(r_3 - 3\sqrt{3}r_8)(1 - C_4) - 8\sqrt{3}r_2 r_4 r_7(r_3{}^2 - r_8{}^2 + r_4{}^2 - r_7{}^2 + 2\sqrt{3}r_3 r_8 + C_4)] \\
& + \Gamma\{8r_3{}^2 C_1 C_2(1 - C_4) - r_7{}^2[2r_4{}^2(r_8 + 7\sqrt{3}r_3 + 1) + 8r_3{}^2(7r_8 + \sqrt{3}r_3 + 1)]\},
\end{aligned}$$

with $C_1 = r_3 - \sqrt{3}r_8$, $C_2 = r_3 + \sqrt{3}r_8$, $C_3 = \sqrt{3}r_3 + r_8$, $C_4 = \sqrt{3}r_3 - r_8$.

APPENDIX E: THE BLOCH VECTORS OF THE TRAJECTORY WITHOUT INITIAL-TO-FINAL STATE COUPLINGS

To obtain reasonable control parameters, the intermediate state $|{}^1E\rangle$ is allowed to be occupied. Without loss of generality, the trajectory characterized by the Bloch vector is designed as

$$\begin{aligned}
r_3 = {} & \sqrt{3}\{[2N(3N + 2)\Gamma^2 + \Omega_p{}^2 - 6\Omega_p \Omega_s + \Omega_s{}^2] + \cos(2\phi(t))[3(\Omega_p + \Omega_s)^2 + 6N\Gamma^2(3N + 2)] \\
& - 4\cos[\phi(t)](\Omega_p{}^2 - \Omega_s{}^2) + 4\sqrt{2}N\Gamma\sin[\phi(t)](\Omega_p + \Omega_s) + 6\sqrt{2}N\Gamma\sin[2\phi(t)](\Omega_p - \Omega_s)\}/(16z), \\
r_8 = {} & \{-[2N(3N + 2)\Gamma^2 + \Omega_p{}^2 - 6\Omega_p \Omega_s + \Omega_s{}^2] - 12\cos[\phi(t)](\Omega_p{}^2 - \Omega_s{}^2) - \cos[2\phi(t)][3(\Omega_p + \Omega_s)^2 \\
& + 6N\Gamma^2(3N + 2)] + 12\sqrt{2}N\Gamma\sin[\phi(t)](\Omega_p + \Omega_s) - 6\sqrt{2}N\Gamma\sin[2\phi(t)](\Omega_p - \Omega_s)\}/(16z),
\end{aligned}$$

in which $\phi(t)$ determines the population on $|{}^1E\rangle$, i.e.,

$$P_2 = \{2N\Omega^2 + 2N^2\Gamma^2(3N + 2) + \sin[\phi(t)]^2[(\Omega_p + \Omega_s)^2 + 2N\Gamma^2(3N + 2)] - \sqrt{2}N\Gamma\sin[2\phi(t)](\Omega_p - \Omega_s)\}/(2z). \tag{E1}$$

Here r_4 is determined by the implicit differential equation $\Omega_c^i(t) = 0$; r_2 and r_7 are the same as in the adiabatic trajectory [r_2 and r_7 in Eq. (C4)]. We consider the adiabatic pulses $\Omega_{p,s}$ like Eq. (11) with

$$\theta(t) = \frac{\pi}{2}\sin\left(\frac{\pi t}{2\tau}\right)^2,$$

and the trajectory with

$$\phi(t) = \frac{\pi}{9}\sin\left(\frac{\pi t}{\tau}\right)^2.$$

Thus, we can numerically determine all the control parameters.

[1] C. P. Koch, M. Lemeshko, and D. Sugny, Quantum control of molecular rotation, Rev. Mod.Phys. **91**, 035005 (2019).

[2] S. Osnaghi, P. Bertet, A. Auffeves, P. Maioli, M. Brune, J. M. Raimond, and S. Haroche, Coherent Control of an Atomic Collision in a Cavity, Phys. Rev. Lett. **87**, 037902 (2001).

[3] S. Hacohen-Gourgy, L. P. García-Pintos, L. S. Martin, J. Dressel, and I. Siddiqi, Incoherent Qubit Control Using the Quantum Zeno Effect, Phys. Rev. Lett. **120**, 020505 (2018).

[4] P. Král, I. Thanopulos, and M. Shapiro, Colloquium: Coherently controlled adiabatic passage, Rev. Mod. Phys. **79**, 53 (2007).

[5] M. V. Berry, Transitionless quantum driving, J. Phys. A **42**, 365303 (2009).

[6] X. Chen, I. Lizuain, A. Ruschhaupt, D. Guéry-Odelin, and J. G. Muga, Shortcut to Adiabatic Passage in Two- And Three-Level Atoms, Phys. Rev. Lett. **105**, 123003 (2010).

[7] Y. C. Li and X. Chen, Shortcut to adiabatic population transfer in quantum three-level systems: Effective two-level problems and feasible counterdiabatic driving, Phys. Rev. A **94**, 063411 (2016).

[8] J. Huneke, G. Platero, and S. Kohler, Steady-State Coherent Transfer by Adiabatic Passage, Phys. Rev. Lett. **110**, 036802 (2013).

[9] B. B. Zhou, A. Baksic, H. Ribeiro, C. G. Yale, F. J. Heremans, P. C. Jerger, A. Auer, G. Burkard, A. A. Clerk, and D. D. Awschalom, Accelerated quantum control using superadiabatic dynamics in a solid-state lambda system, Nat. Phys. **13**, 330 (2017).

[10] M. S. Sarandy and D. A. Lidar, Adiabatic approximation in open quantum systems, Phys. Rev. A **71**, 012331 (2005).

[11] L. C. Venuti, T. Albash, D. A. Lidar, and P. Zanardi, Adiabaticity in open quantum systems, Phys. Rev. A **93**, 032118 (2016).

[12] S. L. Wu, X. L. Huang, H. Li, and X. X. Yi, Adiabatic evolution of decoherence-free subspaces and its shortcuts, Phys. Rev. A **96**, 042104 (2017).

[13] L. Dupays, I. L. Egusquiza, A. del Campo, and A. Chenu, Superadiabatic thermalization of a quantum oscillator by engineered dephasing, Phys. Rev. Res. **2**, 033178 (2020).

[14] R. Dann, A. Tobalina, and R. Kosloff, Shortcut to Equilibration of an Open Quantum System, Phys. Rev. Lett. **122**, 250402 (2019).

[15] G. Vacanti, R. Fazio, S. Montangero, G. M. Palma, M. Paternostro, and V. Vedral, Transitionless quantum driving in open quantum systems, New J. Phys. **16**, 053017 (2014).

[16] S. L. Wu, X. L. Huang, and X. X. Yi, Fast trajectory tracking of the steady state of open quantum systems, Phys. Rev. A **99**, 042115 (2019).

[17] M. S. Sarandy, E. I. Duzzioni, and M. H. Y. Moussa, Dynamical invariants and nonadiabatic geometric phases in open quantum systems, Phys. Rev. A **76**, 052112 (2007).

[18] Xi Chen, E. Torrontegui, and J. G. Muga, Lewis-riesenfeld invariants and transitionless quantum driving, Phys. Rev. A **83**, 062116 (2011).

[19] Xi Chen and J. G. Muga, Engineering of fast population transfer in three-level systems, Phys. Rev. A **86**, 033405 (2012).

[20] A. Baksic, H. Ribeiro, and A. A. Clerk, Speeding up Adiabatic Quantum State Transfer by Using Dressed States, Phys. Rev. Lett. **116**, 230503 (2016).

[21] S. Alipour, A. Chenu, A. T. Rezakhani, and A. del Campo, Shortcuts to adiabaticity in driven open quantum systems: Balanced gain and loss and non-markovian evolution, Quantum **4**, 336 (2020).

[22] L. J. Rogers, S. Armstrong, M. J. Sellars, and N. B. Manson, Infrared emission of the NV centre in diamond: Zeeman and uniaxial stress studies, New J. Phys. **10**, 103024 (2008).

[23] C. E. Carroll and F. T. Hioe, Three-state systems driven by resonant optical pulses of different shapes, J. Opt. Soc. Am. B **5**, 1335 (1988).

[24] Y. H. Issoufa and A. Messikh, Effect of dephasing on superadiabatic three-level quantum driving, Phys. Rev. A **90**, 055402 (2014).

[25] A. Shabani and H. Neven, Artificial quantum thermal bath: Engineering temperature for a many-body quantum system, Phys. Rev. A **94**, 052301 (2016).

[26] J. Zhang, J. H. Shim, I. Niemeyer, T. Taniguchi, T. Teraji, H. Abe, S. Onoda, T. Yamamoto, T. Ohshima, J. Isoya, and D. Suter, Experimental Implementation of Assisted Quantum Adiabatic Passage in a Single Spin, Phys. Rev. Lett. **110**, 240501 (2013).

[27] A. Vepsäläinen, S. Danilin, and G. Sorin Paraoanu, Superadiabatic population transfer in a three-level superconducting circuit, Sci. Adv. **5**, 5999 (2019).

[28] Y. X. Du, Z. T. Liang, Y. C. Li, X. X. Yue, Q. X. Lv, W. Huang, X. Chen, H. Yan, and S. L. Zhu, Experimental realization of stimulated raman shortcut-to-adiabatic passage with cold atoms, Nat. Commun. **7**, 12479 (2016).

[29] J. Kölbl, A. Barfuss, M. S. Kasperczyk, L. Thiel, A. A. Clerk, H. Ribeiro, and P. Maletinsky, Initialization of Single Spin Dressed States Using Shortcuts to Adiabaticity, Phys. Rev. Lett. **122**, 090502 (2019).

[30] A. Barfuss, J. Teissier, E. Neu, A. Nunnenkamp, and P. Maletinsky, Strong mechanical driving of a single electron spin, Nat. Phys. **11**, 820 (2015).

[31] J. P. Tetienne, L. Rondin, P. Spinicelli, M. Chipaux, T. Debuisschert, J. F. Roch, and V. Jacques, Magnetic-field-dependent photodynamics of single NV defects in diamond: An application to qualitative all-optical magnetic imaging, New J. Phys. **14**, 103033 (2012).

[32] J. Klatzow, J. N. Becker, P. M. Ledingham, C. Weinzetl, K. T. Kaczmarek, D. J. Saunders, J. Nunn, I. A. Walmsley, R. Uzdin, and E. Poem, Experimental Demonstration of Quantum Effects in the Operation of Microscopic Heat Engines, Phys. Rev. Lett. **122**, 110601 (2019).

[33] K. Funo, N. Shiraishi, and K. Saito, Speed limit for open quantum systems, New J. Phys. **21**, 013006 (2019).

[34] P. Pietzonka and U. Seifert, Universal Trade-Off between Power, Efficiency, and Constancy in Steady-State Heat Engines, Phys. Rev. Lett. **120**, 190602 (2018).

[35] M. G. Bason, M. Viteau, N. Malossi, P. Huillery, E. Arimondo, D. Ciampini, R. Fazio, V. Giovannetti, R. Mannella, and O. Morsch, High-fidelity quantum driving, Nat. Phys. **8**, 147 (2012).

[36] H. Zhou, Y. Ji, X. Nie, X. Yang, X. Chen, J. Bian, and X. Peng, Experimental Realization of Shortcuts to Adiabaticity in a Nonintegrable Spin Chain by Local Counterdiabatic Driving, Phys. Rev. Appl. **13**, 044059 (2020).